ALMA MATER STUDIORUM
UNIVERSITA' DI BOLOGNA

SCUOLA DI SCIENZE

Corso di Laurea Magistrale in Analisi e Gestione dell'Ambiente

Phytoplankton silica uptake under different artificial upwelling conditions in the Canary Islands

Tesi di Laurea in Botanica Marina Applica

Relatrice: Chiar.mo Prof. Rossella Pistocchi

Correlatore: Dr. Mar Fernández-Méndez

Prof. Maria Antonia Colangelo

Presentata da:

Andrea Timoncini

VII Sessione, Anno Accademico 2019-2020

Abstract

Climate change is affecting pelagic ecosystems with repercussions on fish production. In particular, global change is increasing oceanic temperature and stratification with decrease in nutrient input in euphotic layer leading to a decline in primary production. The mesocosm-based project Ocean Art-Up, conducted in Gran Canaria, is aimed to increase fish production and to enhance carbon sequestration through an artificial upwelling system. Diatoms dominate the phytoplankton community in upwelling systems and they need to take up silicates to grow. The abundance and nutritional value of diatoms determine the fate of phytoplankton biomass with transport to the upper level of the pelagic food web or to the deeper layer of the ocean with potential carbon sequestration. Here, data about experiments performed in 2018 and 2019 are reported. The first mesocosm experiment investigated the differences between pulsed and continuous upwelling mode, while the second experiment was conducted with a gradient in Si:N ratio along the mesocosms. The phytoplankton community takes up and incorporate silica about at the same rate in continuous mode, while in pulsed mode its peak occurred only after the deep-water addition. The diatom silica content is not affected by mode and amount of water added but by the Si:N ratio. Diatoms grown in an environment with high Si:N ratio values show higher abundance, biogenic silica production, silica uptake and silica content than the ones that experienced low Si:N values. In addition from literature, euphotic zone rich in silicate may produce high silica containing-diatoms who will produce repercussions on copepods community regarding feeding, hatching and growth, thus continuous upwelling with high Si:N ratio favours diatoms who will tend to sink and to be converted by copepods into fecal pellet rich in silica with increasing in potential carbon sequestration. Fish production may increase with continuous artificial upwelling showing low Si:N values.

Table of Contents

1. Introduction

1.1. Marine pelagic ecosystems

A standard feature of a marine pelagic ecosystem is the presence of abiotic and biotic factors which interact between them. This environment, beside being important for the reach biodiversity, is important also for human beings for its ecosystem services.

1.1.1 Abiotic factors

Abiotic factors exert a bottom up control, so they could be considered as the base of marine ecosystem given that they drive its structure. They consist in temperature, salinity, nutrients, light and seasonality. The light is the source of energy which allows the creation of biomass by primary producers, it also determines the depth at which they can live. This environment is called euphotic zone and it extend to the first 100-150 m depth. The temperature drives the development of the marine ecosystem by selecting which type of organisms can live in it. The temperature varies according to latitude, season and depth. The maximum temperature is recorded at the surface, in the equatorial zones, with decreases by about 1 °C for each degree of increase in latitude. The temperature also

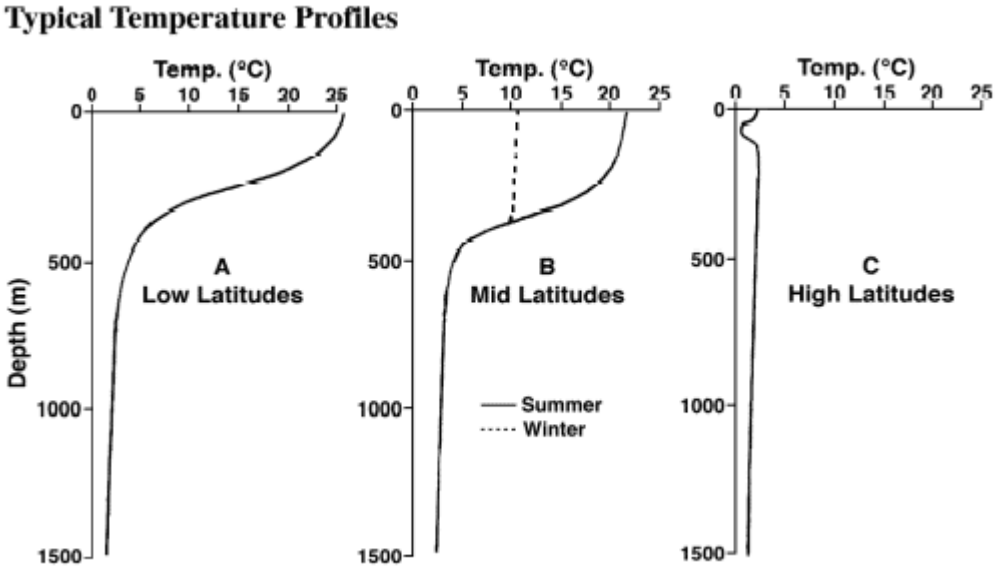

Figure. 1.1. This shows the typical temperature profile for low, mid and high latitude marine basin.

decreases with depth, in fact between 200 and 1000 m there is a sudden decrease in temperature: this layer is called thermocline, below it the temperature stabilizes in depth

at values close to 0 ° C. The upper layer is called mixed layer where the wider changes in temperature occur.

Salinity with temperature and pressure determine the oceanic circulation that in turn affects the distribution of the nutrients.

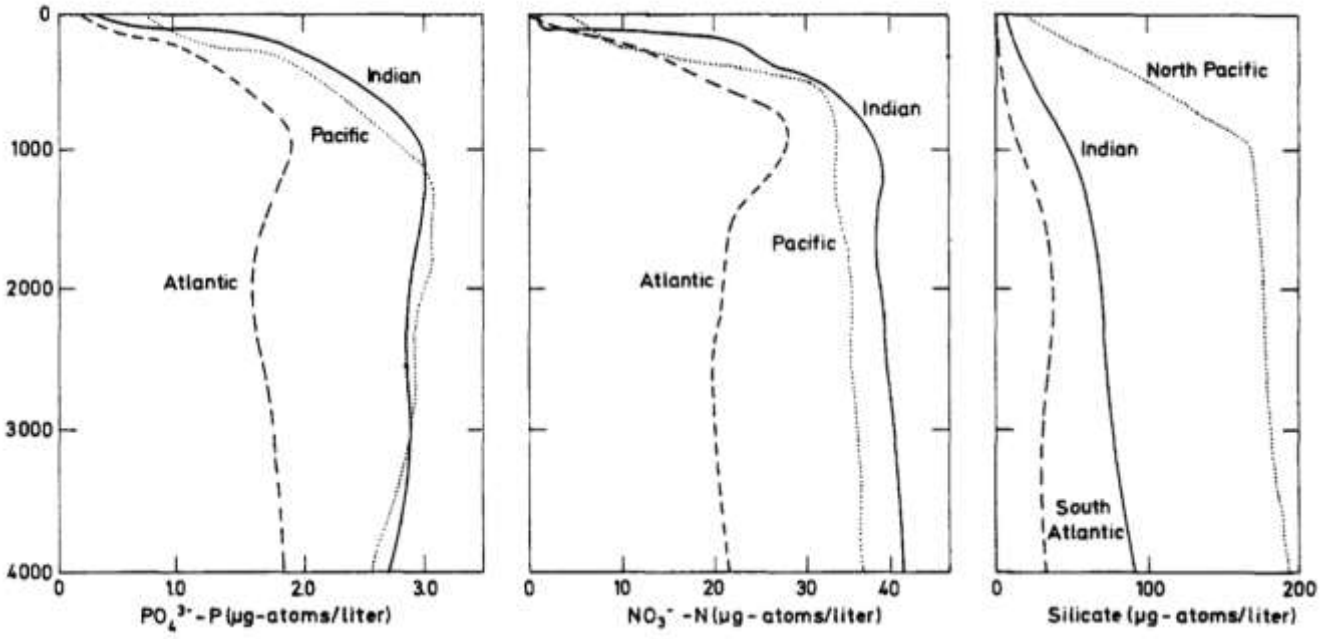

Figure.1.2. It shows the vertical distribution of phosphate, nitrate and silicate in the three major oceans. (from Richards, 1968 and RC-Dugdale 1972).

Nutrients are essential for the growth of primary producers. The most important are nitrate, phosphate and silicate. They are usually distributed along the depth of the water column with a peak around 1000 meters, after which their concentration tends to decrease due to bacteria activity and it shows stability thank to deep water oceanic circulation. Nutrients are taken up by primary producers mostly according to the REDFIELD ratio of 106 C:16 N: 1P, this relationship is kept also for the regeneration ratios occurring in water below the euphotic zone (Redfield et al. 1963). Taking into account also the utilization of silicate by diatoms it becomes 106C: 16N: 15Si: 1P (Brzezinski, 1985). In Fig. 1.2 it is also possible to note the different nutrient pattern between the three ocean basins. (Dugdale, 1972). In every temperate basin seasonality occurs with changes in the structure of ecosystem. In Canary Islands the typical water is oligotrophic with a seasonal thermocline, which separates low-nutrient, low-Chlorophyllα surface from deep nutrient-rich waters (de León and Braun, 1973; Cianca et al., 2007). During Spring water becomes warmer than in winter and its stratification increases throughout summer with strong winds. It continues until Autumn when a decrease in temperatures occurs.

The mixed layer is deep and cold in the end of winter (March) due to winter convection and low temperatures that produces the consequent mixing of the water. (Pelegrı´ et al., 2005) This pattern is specifically due to the circulation of the sea water as also resulting from oceanic thermohaline circulation and wind pattern. It is characterized by eastward flowing Azores Current which splits into several southward branches. (Schimitz and McCarteney 1993). When in the end of winter, thanks to wind, temperature and oceanic circulation, the deep water goes up, an upwelling occurs which brings rich-nutrient water from the depth to the top layer allowing the increase in productivity.

1.1.2. Biotic factors

The biotic factors are those related to the food web and, regarding marine ecosystems, from the bottom we may find phytoplankton, zooplankton, fish and other more developed organisms while, as remineralizer, there are the bacteria. Organisms that could influence silica uptake are phytoplankton with diatoms, zooplankton and bacteria. Within phytoplankton we can find cyanobacteria, silica-encased diatoms, dinoflagellates, green algae, and chalk-coated coccolithophores. They have in common the capacity to perform photosynthesis, thus they represent the primary producers. Each group has particular characteristics: cyanobacteria (P. Zehr, et al 2001) are involved in nitrogen fixation, diatoms are the most abundant primary producers and involved in silica cycle, as explained by Hildebrand (2008), dinoflagellates are at the second place as primary producer and some of them are known for their toxin production (Taylor & Pollingher, 1987), coccolithophores get importance from the production of calcium carbonate shell (Tyrrell & Young, 2009).

Specifically, Diatoms represent the most predominant phytoplankton organisms contributing to the global carbon fixation and to the silica cycle. In particular, they account for 40-50% of the total primary production in the ocean (Nelson et al., 1995, Tre´guer et al., 1995; Mann, 1999; Smetacek, 1999; Tre´guer and Pondaven, 2000). These two features make diatoms the major regulators of carbonium and silicon cycle in the ocean and with repercussions on the entire biogeochemical cycles. The phytoplankton community is top-down regulated by zooplankton who grazes the first. Each zooplankton group has preference in prey selection. In high efficient food web, as in the upwelling ecosystem, diatoms are eaten by copepods, and then they are top-down controlled by fish (U. Sommer et al, 2002). In this configuration many groups of bacteria have the role of nutrient remineralizers, thus they convert the dead organic compounds into inorganic

ones in order to recycle the matter. Phytoplankton will pick up the inorganic compounds as nutrients. Pelagic food web, with its interactions, may influence the growth of diatoms, that results in changes in silica uptake rate.

1.2. Marine carbon and silica cycles

Carbon and silica cycles in ocean get importance because they are involved in important processes like biological carbon and silica pump and each minor changing determines a big change in the marine ecosystem. Most of the carbon in the oceans is present in an ionic form, not in gaseous CO_2 form. This is due to the dissolution of CO_2 in seawater which reacts with water forming carbonic acid, this dissociates into bicarbonate with releasing of proton. Moreover, bicarbonate releases carbonate ion and a proton. This process of CO_2 uptake and dissolution leads to a decrease of the pH value in seawater. It is interesting how, of the total amount of dissolved inorganic carbon (DIC), only 1% remains in the gaseous form of CO_2, the most part is in the form of $HCO3^-$ (~ 90%) at typical seawater pH (Zeebe and Wolf-Gladrow, 2007). Carbon is transported from the surface to the deep ocean by physical and biological carbon pump as explained by Volk and Hoffert (1985). The physical pump consists in transport of carbon mediated by global differences in sea water temperature and salinity, thus affecting CO_2 solubility. CO_2 is more soluble in cold water thus it can sink in cold and dense water masses at high latitudes to be transported to the depth. The upwelling occurring at lower latitudes can cause the release of that CO_2. On the contrary, the biological carbon pump is due to phytoplankton located in the oceanic surface. It includes the soft-tissue pump and the carbonate counter pump. The first one is due to the capacity of autotrophs to convert dissolved inorganic carbon (DIC) into organic matter mostly for the process of photosynthesis but also minor processes are involved. This leads to a decrease in CO_2 concentration in oceanic surface. The organic carbon, also called particulate organic carbon (POC) is largely remineralized in the surface sea water, with realising of CO_2. Another fate of POC is the sinking to the deep ocean, determining the carbon export, this can in part be converted to DIC and in minor part constitutes part of the sediment. The carbonate counter pump due to calcifiers leads to a decrease in DIC with the sinking of biogenic carbonate. The ratio between uptake and export determines the net effect of the biological carbon pump, which nowadays favours the uptake of CO2 from the atmosphere, as written by Sarmiento et al. (2002).

The marine silica cycle gets importance from its relation with marine primary production, the efficiency of carbon export to the deep ocean and the inventory of carbon dioxide in the atmosphere. Silicon inputs come from continent through rivers, in the form of dissolved silicon and biogenic silica, and through eolian inputs. In the ocean, hydrothermal input occurs carrying dissolved silicon. Silicon is utilized by producers which convert dissolved silica into biogenic silica. This process is supported in the photic layer by siliceous organisms, which are diatoms for the most, silicoflagellates and radiolarians. (Nelson et al.1995) Biogenic silica flux is in part exported to the deep ocean and in part recycled in the surface of the ocean.

1.2.1. Primary productivity

Primary producers convert inorganic carbon into organic carbon compounds. The rate, in the ocean, at which inorganic carbon in the form of DIC or atmospheric CO2 is converted in organic matter is called primary productivity. (K. E. Frey et al. 2017) Primary production is sustained by phytoplankton and photoautotrophic bacteria, and it represents the basis of the entire marine food web. Primary production requires photosynthesis process, as the producers form the base of the entire food web. Oceans, through this process, play an essential role in biogeochemical fluxes, in fact it provides half of the global net annual photosynthesis. (Müller-Karger et al. 2005)

Chlorophyll-*a* plays a fundamental role in photosynthesis process as it represents the pigment by which it can occurs. Algal pigment chlorophyll (e.g. chlorophyll-*a*) is measured since it can be a proxy for the quantity of algal biomass. The rate of chlorophyll production represents the growth rate of algal community besides the primary productivity.

Particulate organic carbon (POC) is another indicator of primary productivity in the euphotic layer of the ocean as it includes living material (phytoplankton, zooplankton, bacteria) and detritus. (MervFingas 2019)

Primary production is heterogeneously localized around oceanic surface and depth. Its spatial distribution is due to bottom up and top down control. Light and nutrients availability are part of bottom up control while in top down control we may find predation from zooplankton. (C. M. Moore et al., 2013).

Primary productivity is dominated, in particular during upwelling event, by diatoms which incorporate a great amount of carbon while they build up their silica wall.

1.2.2. Silica uptake by diatoms.

Diatoms are the most predominant siliceous organisms into the marine environment with their silicified cell wall, they precipitate silicate in the form of hydrated amorphous silica in particular structures called frustules. The structure of silica cell wall is genetically controlled, and under physiological control to avoid uncontrolled autopolymerization of silica. There are two undissociated silicic acid forms which are taken up by diatoms: $Si(OH)_4$ which comprises about 97% of the dSi (dissolved silica) in seawater at pH 8.0, and $SiO(OH)_3^-$ which comprises most of the remaining 3%. (Ingri 1978, Stumm and Morgan 1981) Most diatoms species respects this proportion, so they mostly transport undissociated silicic acid (Del Amo and Brzezinski 1999).

It is clear now that diatoms transport silicon at a specific rate of uptake and in addition the specific Si uptake rate is cell-division-dependent, it follows Michaelis-Menten or Monod (1942) saturation functions. The transport/uptake of silicic acid may occur with one of three different pathways: surge uptake, internally controlled uptake and externally controlled uptake. Once transported, silicon has to be deposed, this happens thanks to the membrane-bound silica deposition vesicle, (SDV), called silicalemma. In addition, cell growth cycle and the deposition of new silica valves are closely related (Brzezinski 1992). Thus, deposition of the entire frustule occurs during one continuous segment of time beginning just before division and it ends just before daughter cell separation. Specifically, it has been found that there are two universal arrest points among diatoms: one at the G1/S boundary and another during G2/M associated with construction of new valves (Darley and Volcani 1969, Vaulot et al. 1987, Brzezinski et al. 1990).

The quantification of silica deposition rate can be done using the biogenic silica measurement which represent the concentration of opale made from diatoms, while the quantification of silica uptake rate can be done using dissolved silica.

Many factors contribute to regulate the silica uptake, the most important is the silicic acid availability, or better the Si:N ratio. Diatoms show higher biogenic silica precipitation and higher growth capacity with higher Si:N ratio, in fact low ratio favours non-siliceous algae. (Sommer 1983,1994,1996,1998; Tilman1982; Tilman et al. 1986).

1.2.3. Carbon and silica export

Nowadays in the ocean, carbon and silica can be exported through the biological pump, which is represented for the most by the photosynthetic activity of diatoms. The great

growth ability of diatoms, in response to nutrients availability, drives the export of particulate organic carbon from the euphotic zone to the deep waters with high correlation with the flux of particulate silicate. This is due to the simultaneously precipitation of silicate and fixation of carbon made by diatoms. (All et al. 2005) In this way a positive relationship at a global-scale between diatom productivity and organic carbon burial occurs (Fatima Abrantes et al. 2016).

1.2.4. Carbon transfer from phytoplankton to fish

Carbon can be exported through biological carbon pump to upper trophic levels. The most efficient food web is made up of phytoplankton, dominated by diatoms, zooplankton, in particular copepods, and then fish. This could be the ideal situation, in reality copepods eat ciliates, dinoflagellates and diatoms. For long time it has thought that diatoms were the most relevant food for copepods, and as reported by Cushing (1989), in diatom blooms a very high copepod productivity can occur, resulting in higher carbon transfer to the upper trophic levels.

Nowadays, there is an intense debate due to the toxic effects and low nutritional quality of diatoms (Poulet et al., 1994; Ianora et al., 1995; Jonasdottir & Kiørboe, 1996, Jonasdottir et al., 1998; Irigoien et al., 2002; Dutz et al., 2008). This is due to the possibility that some diatoms may produce toxic substances such as aldehydes (Miralto et al., 1999; Wichard et al., 2008), moreover, they do not provide suitable fatty acid profiles for egg production for copepods (Jonasdottir & Kiørboe, 1996; Ban et al., 1997). In addition, Dutz et al., 2008 shows that diatoms can be difficult to be digested due to their frustules. Thus, copepods may prefer other phytoplanktonic species besides diatoms when they release toxin or show intense silicification in their frustules.

1.3. Ecosystem services

Oceanic ecosystems provide goods and services. One of the most important good from marine ecosystem for humans is fish production. The current global fish production is about 160 million of tons per year (in 2004), including in land production that account for 23%, so the most part (77%) comes from ocean. Moreover, capture fisheries account for a 68% of the total, thus only 32% come from aquaculture. The quantity of fish produced depends on the net primary production (NPP) and only up to 30% of biomass at each trophic level pass through the ecosystem chain. One of the most important service is the carbon sequestration, by which atmospheric CO_2 is stored into sea water or better in its

sediment. These relevant benefits are linked each other and moreover are now under pressure due to changing in the ocean due to climate change and overfishing. (Barbier, 2017)

1.4. Climate change

Report of IPCC of the year 2014 well explained the causes and effects of climate change. In particular, the temperatures are rising due to human activity, which increases the climate-changing gases concentration in atmosphere. The result is the warming of the atmosphere, since 1950, and also of the ocean with many side consequences. Moreover, from Special Report: ”Global Warming of 1.5°C”, in 2017 the Earth reached a warming of approximately 1°C (likely between 0.8°C and 1.2°C) higher than pre-industrial levels, with increasing rate of 0.2°C (likely between 0.1°C and 0.3°C) per decade (High confidence).

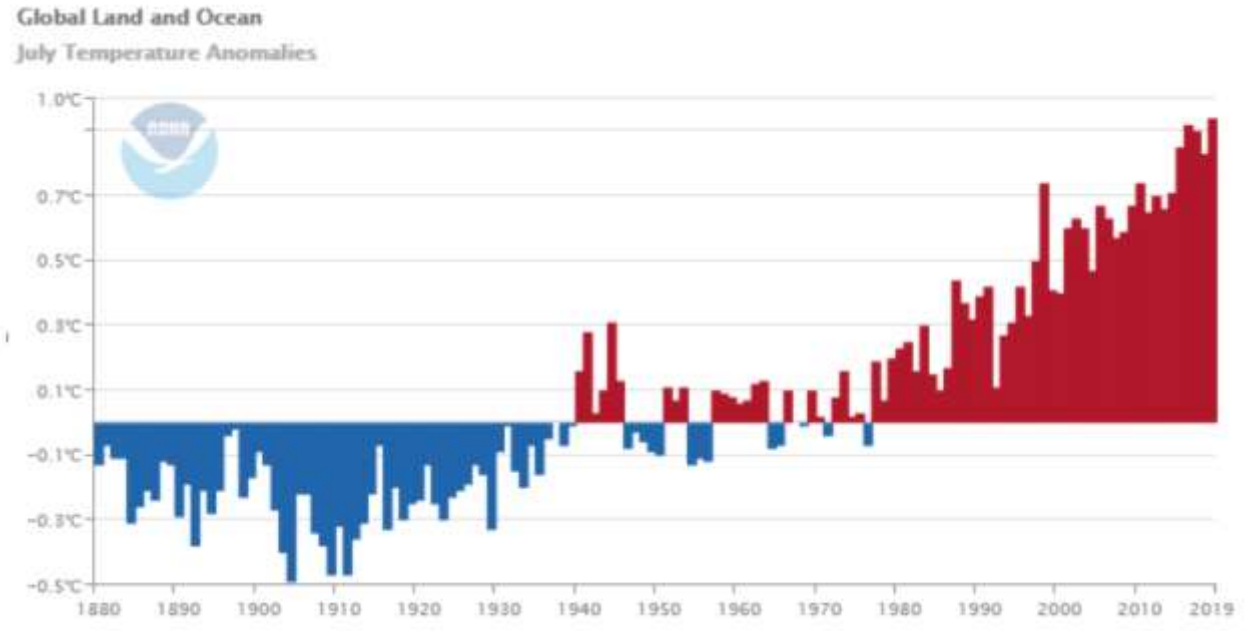

Figure 1.3. July global sea surface temperature anomalies from 1880 to 2015 with superimposed linear trend (Base period 1951–1980), red positive, blue negative. From: http://www.ncdc.noaa.gov/cag/time-series/global/globe/ocean/ytd/12/1880-2016.

This high rate of temperature rising has brought to decide an upper limit in temperature and how to avoid it. From the same report, scientist fixed that at 1.5°C. In addition, in the “IPCC special report on carbon dioxide capture and storage” we can find description of sources, capture, transport and storage of CO_2, with evaluation of oceanic storage as mitigation action.

The oceanic surface (the upper 75 m) warming on a global scale is about 0.11°C [0.09 to 0.13] per decade over the period 1971 to 2010 (IPCC report 2014). This warming is leading to many side effects on marine ecosystem. Those related to thus thesis are

deoxygenation and nutrient limitation due to the warming which in association with ocean acidification may cause many negative effects on marine life with impact on fish harvesting. (IUCN)

1.4.1. Effects of global warming on diatoms and on nutrient availability for them.

Nowadays the temperature rising in the ocean is leading to a higher sea water stratification, that coupled with the warming, bring to a deoxygenation and in particular to a decline in nutrient concentration in the euphotic layer. (O'Connor et al., 2009; Diaz and Rosenberg, 2008).This scenario negatively affects diatoms productivity since the nutrient availability decreases with the increasing in water column stratification, in fact, according to Steinacher et al. (2010) primary production tends and will tend to decrease from 2% to 20% by 2100 in mid and low latitudes due to the reduction of nutrient input to the euphotic zone. Moreover also models like this of L. Bopp et al.,(2005) found similar results, in particular the Nord Atlantic Deep Water circulation(NADW) will be reduced by almost 50% with $4xCO_2$, (that corresponds to global average surface warming reaches +3.2°C) with increased oceanic vertical stratification and decreased convective overturning. In addition, from this model it is clear that the increasing in vertical stratification leads to more oligotrophic condition and as ecological consequence the decline of big diatoms in favour of small phytoplankton. In fact, they found a decrease in contribution of diatoms to the total chlorophyll, from 0.27 at $1xCO_2$ to 0.24 at $4xCO_2$. This change in phytoplankton composition, due to climate change thus more stratification and nutrient and carbon recycling in the surface ocean influences export ratio with a reduction of 25% at $4xCO_2$ while primary production decreases by only 15%. The reduction in export ratio leads to a less atmospheric carbon uptake, since the export of organic carbon is decreased and it is not compensated by the decline of upward inorganic carbon flux. This, in part, is due to the reduction in phytoplankton dimensions, which determines a minor sinking rate. (L. Bopp et al., 2005) All of these causes and consequences lead to a less nutrient availability for diatoms and thus to a decrease in relative abundance of them in the future ocean.

1.4.2. How silica is changing in the ocean.

Silica concentration in ocean is reported to change. This is due to a decline in river flux by building of dams which leads to a storage of a third of the global sediment discharge. (Paul J. Treguer and Christina L. De La Rocha, 2013). Dissolved silica, biogenic silica and other forms are therefore trapped. (Humborg et al. 1997, 2000; Ittekkot et al. 2000)

Moreover, the great amount of nitrate and phosphorus used in agriculture leads to an increase in biogenic silica production in river with a decline of dissolved silica in coastal environment as consequence. This leads to a decrease in diatoms importance in coastal areas (Turner & Rabalais 1994, Nelson & Dortch, 1996, Humborg et al. 2000). A further consequence is a higher probability in occurrence of harmful algal bloom episodes. In addition to this, in the open ocean, upper water warming leads to higher stratification resulting in lower dSi inputs from the waters below and, consequently, to a decrease of biogenic silica and primary production with repercussion on carbon and silica export. (Paul J. Tr´eguer and Christina L. De La Rocha, 2013)

1.5. Artificial upwelling as a solution for climate change

Artificial upwelling can mimic the effects of natural upwelling, thus enhancing primary production. This was the result of an artificial upwelling experiments (Aure et al., 2007; Giraud et al., 2015; Handå et al., 2013; McAndrew et al., 2007; McClimans et al., 2010; Strohmeier et al., 2015). Artificial upwelling could be a solution or a mitigation action against climate change because it can reduce the decline in primary productivity, in fact it can increase the biological carbon pump in oligotrophic systems. In this way, this new approach can be a way to solve problems due to overfishing and make the fishing more sustainable. Artificial upwelling can also have repercussion on carbon exchange, in fact it could increase carbon sequestration if it properly performed. The risk is that deep water is rich in DIC, thus this carbon could be release into the atmosphere when it has brought to the surface. Nowadays, we still have very few experiments on artificial upwelling and many models which estimates the possible carbon sequestration. From these models and experiments, many uncertainties and doubts have to be solved on carbon sequestration. (Bauman et al., 2014; Keller et al., 2014; Lenton and Vaughan, 2009; Williamson et al., 2009; Yool et al., 2009). From the rising of deep cold water to the oceanic surface there can also be another useful effect for the climate, in fact the cold water can reduce the temperature of the air close to the oceanic surface. As last positive application, artificial

upwelling can utilize the thermal gradient to produce renewable energy. This system is called OTEC (ocean thermal energy conversion) power plants (Fuller, 1978). Its feasibility is still far away due to high costs and technical feasibility. The figure below shows a hypothetical artificial upwelling system. (Fig. 1.4) The depth of the system depends on the characteristic depth where high concentration in nutrient can be found.

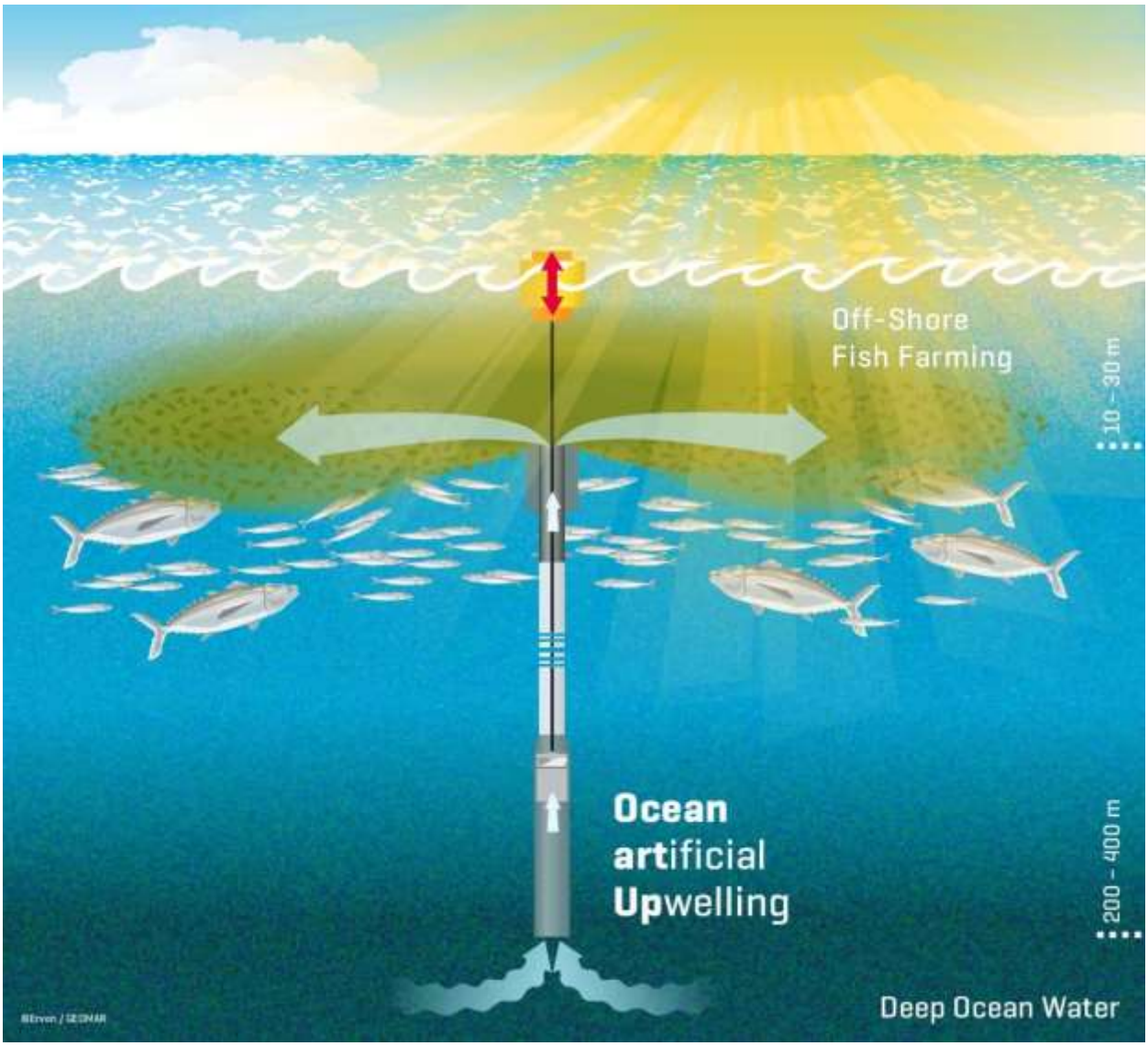

Figure 1.4. Final model of artificial upwelling system, thought by GEOMAR group.

1.6. The Canary Islands: why are they a good location for an artificial upwelling experiment?

Canary Islands are surrounded by oligotrophic water. This area increases its productivity when upwelling of deep water occurs. This is mostly driven by eddies at mesoscale (Arístegui et al., 1997; Basterretxea and Arístegui, 2000). When it happens water from hundreds meters depth goes up, reaching the surface and carrying high concentration of nutrients. This typically oligotrophic water makes this area ideal for upwelling experiments aimed to increase fish production and carbon sequestration by enhancing biological pump and thus the primary productivity.

2. Research approach

Mesocosm experiments:

In order to evaluate silica uptake by diatoms and its repercussion on fish production and carbon sequestration and thus on the effectiveness of artificial upwelling, we utilized two different upwelling system experiments composed of mesocosms. In the first one of 2018 9 mesocosms were utilized while for the second experiment of 2019 8 mesocoms. In the first one a gradient in percentage of deep-water addition was created, in the second one there was a gradient of Si*. For Si* we mean the difference in concentration between dissolved silica and dissolved inorganic nitrogen. Thus, in this way through the mesocosm approach, the natural upwelling occurring with the addition of deep seawater was mimed. (Aure et al., 2007; Giraud et al., 2016; Handå et al., 2013; McAndrew et al., 2007; McClimans et al., 2010; Strohmeier et al., 2015)

Deep water has a high concentration of the main inorganic nutrients: phosphate, silica and nitrogen, thus its addition means an increase of their concentration. In the oligotrophic system in which we decided to develop the experiment, Gran Canaria, the addition of nutrient-rich deep water results in increasing in primary productivity through the biological carbon and silica pump (Aure et al., 2007; Giraud et al., 2016; Handå et al., 2013; McAndrew et al., 2007; McClimans et al., 2010; Strohmeier et al., 2015). In particular from literature, the addition of silica tends to enhance the growth of diatoms and, given that they represent the most important and abundant phytoplankton group, primary productivity will increase as well. (Nelson et al., 1995;Mann, 1999; Smetacek, 1999)

Today, we don't have yet many studies regarding transfer efficiency and, in particular, the fate of diatom biomass after deep water addition in oligotrophic water, in addition controversial results were also obtained.(Poulet et al., 1994; Ianora et al., 1995; Jo ´nasdo ´ttir & Kiørboe, 1996, Jo ´nasdo ´ttir et al., 1998; Irigoien et al., 2002; Dutz et al., 2008)

Motivation and expectations:

Artificial upwelling miming the natural upwelling brings nutrient-rich deep water to the euphotic zone, resulting in increasing in primary production. Nowadays a decline in primary production in the ocean is occurring due to climate change with consequences on marine ecosystem and also on human population in particular on those close to the

coast. The use of this technique can show a sustainable way of increasing fish production and could be a mitigation action against climate change.

Thanks to that, we expected an increase in nutrients concentration followed by enhancement of primary production. As one of the results of the increasing in nutrient concentration is the increase in diatoms abundance, silica uptake is also expected to increase and, in case, at some point to reach a plateau. From the increasing in diatoms abundance we also expect a more efficient carbon transfer to higher trophic levels but an increasing in sinking may be expected as well (Eppley and Peterson, 1979; Allen et al., 2005). The higher sinking due to biological carbon pump will result in increasing in carbon sequestration (Fatima Abrantes et al., 2016). It is not yet clear whether an improvement in marine trophic chain or CO_2 sequestration is favoured with an increase in deep water addition and Si* value. (Allen et al., 2005)

Scientific questions

The two experiments have in common the objective to study the ecological feasibility of artificial upwelling system in increasing ocean productivity and carbon sequestration.

Specifically, this Master Thesis evaluates the silica uptake under different upwelling conditions.

The main scientific questions of this study are:

- Is silica uptake higher in pulsed or in continuous upwelling?
- Does increasing Si*(Si*=[Silicate]-[Nitrate]) enhance the silica uptake?
- Does the amount of deep water added and the N:Si ratio affect the biogenic silica/ diatom abundance ratio?

To answer to these questions, two different experiments were conducted by the Riebesell team from GEOMAR Helmholtz Centre for Ocean Research Kiel, in Taliarte, Gran Canaria, the first one in November-December 2018 with 38 days of experiments and the second one in September-October 2019 with 35 days of duration. These experiments have in common the particularity of including in the mesocosms a small pelagic food web, which represents the local food web.

I joined the Team in 2019 experiment as a Master Student, and took part to the sampling and filtrations for environmental DNA and fatty acids, I measured silica uptake using the fluorescent dye (PDMPO) method and helped with the primary productivity measurements using 13C stable isotopes although these measurements are still being performed so the data will not be available for the thesis. I performed data analysis for both experiments regarding dissolved silica, biogenic silica, chlorophyll-a and diatom abundance.

3. MATERIALS AND METHODS

3.1. Mesocosm field campaigns

Two similar experiments were set up to answer the questions reported in the research aim; they are both included into the framework of the ERC project “ocean art up” in collaboration with Plataforma Oceánica de Canarias (PLOCAN). The first one was conducted in autumn 2018 while the second during the late summer and early autumn 2019 in Gran Canary Island but in different locations. Both experiments show in common artificial upwelling system obtained with mesocosm experiment.

3.1.1. Different upwelling intensities (KOSMOSGC2018)

In 2018 the experiment took place from November 6th to December 13th 2018 in Gando Bay (27˚ 55’ 41” N, 15˚ 21’ 55” W), northeastern Gran Canaria (Canary Islands) (Fig. 3.1).

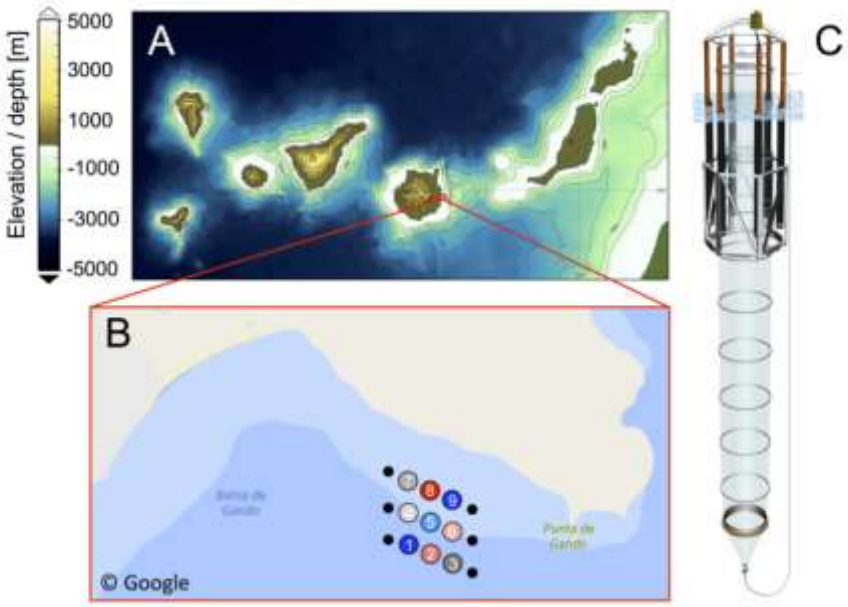

Figure 3.1. Figure taken from Taucher et al. (2017) showcasing the location where mesocosms were deployed in Gando Bay, northeastern Gran Canaria (Figure 3.1A and B) and the structure of one of the 9 KOSMOS used during the experiment (Figure 3.1C).

This area has been chosen due to the influence of the subtropical North Atlantic gyre and, to a lesser extent, the Canary Current, and it shows a predominant oligotrophic condition (Barton et al., 1998; Arístegui et al., 2009).

3.1.1.1. Experimental set-up

The study was conducted utilizing 9 “Kiel Off-Shore Mesocosms for future Ocean Simulations” (KOSMOS). Each mesocosm contained a 14-meter-deep water column, containing approximately 40m³ of ocean water. More details on mesocosm infrastructure, deployment and maintenance can be found on Riebesell et al. (2013).

Mesocosm bags were left open and submerged for 2 days after mooring in order to get from the surrounding water the typical species amount and diversity of the region.
The duration of the experiment was 38 days in total, developed in November and December 2018.
We tested two different upwelling regimes: pulsed, consisting of a single deep-water addition on 4th day; and continuous, in which regular deep-water addition was performed from t4 onwards every 4 days.

In each group of treatments, we have developed an increasing gradient through four mixing ratios of deep to surface water, one per mesocosm. For the pulsed treatments these were 7.2%, 13.5%, 25% and 44%, while for the continuous treatments they were 0.9%, 1.8%, 3.6% and 7.2%. Taking into account the quantity of deep water added, each continuous treatment experienced the same amount of deep water by the end of the experiment as its complementary pulsed treatment, while one mesocosm was kept as untreated control, the mesocosm number 5.

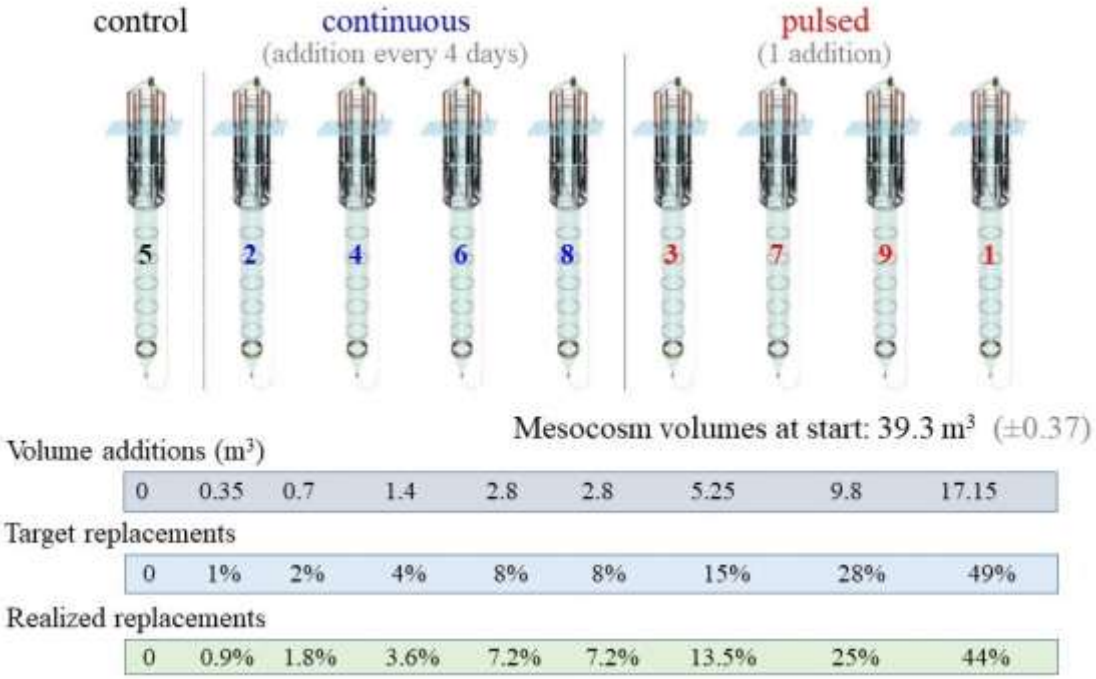

Figure 3.2. Schematic representation of the experimental design showcasing the two artificial upwelling regimes, continuous and pulsed, and deep-water mixing ratios. Deep water mixing ratios are expressed both in terms of ideal deep-water volume addition and percent mesocosm volume replaced, and realized percent mesocosm volume replaced after volume determination through salt addition. Figure courtesy of Ulf Riebesell.

Artificial upwelling simulation has been conducted with an exchange of water between inside mesocosm and deep water collected. This was done by first removing the volume corresponding to the mesocosm's assigned treatment, and then adding the same amount of deep water.

Water was removed from mesocosm using a peristaltic pump (KUNZ SPF60), which pumps water in pulses in order to maintain a constant flow rate of 14m³/h. It was important that the flow was constant in order to reduce the damage inflicted to organisms that were pumped out, which were collected over a 55µm mesh sized net in order to account for community dilution. Deep water was afterwards introduced using the dive pump. It was also used to collect the deep water from the open ocean.

During both water removal and deep-water introduction, a hose was connected to a device called the "spider", in turn attached to a sampling line in order to lower it down and pull it back up at a constant speed repeatedly over the duration of the procedure. The "spider" consists of a central cylinder with multiple openings on its sides. Plastic tubes,

about 1cm in diameter and of variable lengths, are attached to these openings. This device is necessary because it allows a homogeneous water removal, allowing a proportional dilution of all members of the plankton community, and introduction.

Deep water needed to be collected, its collection was carried out using a modified version of the deep-water collection system described by Taucher et al. (2017). The collection took place on October 26th and November 28th and was deployed at east of Telde (Gran Canaria) aboard the Spanish vessel J-SOCAS. In this case, the collection system did not include the water-intake device, but instead was associated to a stainless steel dive pump (Grundfos SP17-5R). The collection has been made at a depth around 330 meters on the first collection and 270 meters in the second one, this was due to the length of the hose connecting the pump to the collector bag.

The changes produced a new design that is a change in the collection protocol itself. The collection bag remained at the surface, while the pump was lowered to the desired depth, where it works at an average flow rate of 18m³/h.
The first collection took place at N 28°00'3.528" W -15°07'9768", and 100m³ of deep water were collected, while during the second collection, which began at N27°57'18.504" W-15°18'1.08", 40m³ were pumped. In both cases the vessel drifted with stopped engines in a southwesterly direction during collection.
The water needed to show similar concentration in nutrients respect that at 700-meter-depth to be classified as "deep water", thus once the deep water has been collected, it follows a manipulation process in that the nutrient ratio and amount are brought to that of 700-meter-deep water off the Canary Islands. It has been selected this type of water mass because in a follow-up field validation experiment off the Guinea Dome, southeast from Cape Verde, deep water of similar nutrient levels as the 700-meter-deep water off the Canaries will be used.

Prior to conducting any manipulation, we measured nutrient concentration using an auto-analyzer (QuAAtro, Seal Analytical) in order to determine the amount of each nutrient required to achieve the desired concentrations of 12.5 µmol Si/L, 25 µmol N/L and 1.67 µmol P/L. Then, to get the expected concentration of nutrients, stock solutions of nitrogen, phosphorus and silicon were prepared and then mixed into the deep-water bag.

The first deep water collected showed draw-down of nutrients, mainly of N and P. It could be due to bacteria consumption, thus flow cytometry analyses of water samples took place with no significant increase in bacterial numbers through the water column, but we

did not take in consideration bacteria on the collector bag, who could also have been responsible. In this way nutrients had to be manipulated twice, first after collection on the 5th of November, and a second time on 16th of November.

3.1.1.2. Timeline

This experiment started on 6th of November and it ended on 12th of December. The duration of the experiment was 38 days in total, it began with the closing of the sediment traps on t0 (November 6th).

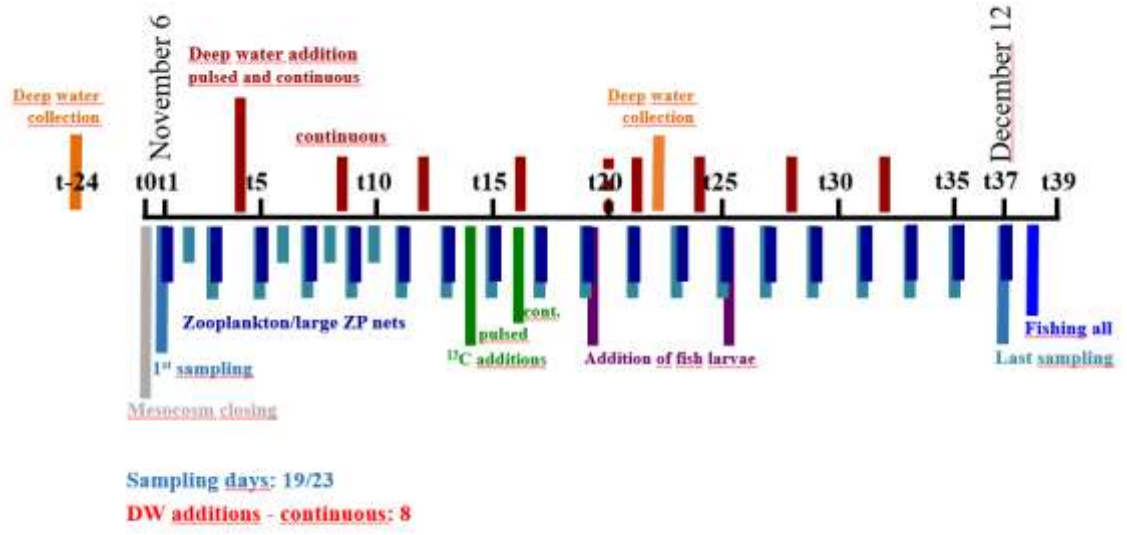

Figure 3.3. Schematic representation of the different activities carried out throughout the duration of the experiment. These include deep water collection (orange), deep water addition (red), mesocosm closing (grey), regular sampling, which includes sediment trap and IWS sampling, and CTD casts (light blue), zooplankton net sampling (dark blue), ^{13}C enrichment for trophic transfer efficiency (green), fish larvae additions (purple), and final fishing of the whole mesocosm (blue).

3.1.1.3. Sampling

The most physical, chemical and biological parameter were sampled every second day throughout the duration of the experiment, few every third day or differently. In particular the sampling took place the first days after mesocosm closure (t1 to t3), when mesocosms were sampled daily to achieve a good baseline, and the days following the first and

second upwelling simulation (t5 to t10), after which the planktonic community was expected to rapidly respond to the deep-water introduction (Figure 3.3).

Water samples were collected using depth-integrated water samplers (IWS), which take up a total volume of 5L uniformly over the desired depth range of 13 meters. These were operated as described in Taucher et al. (2017) in order to sample for dissolved inorganic carbon (DIC), inorganic nutrients (nitrate and nitrite, ammonium, phosphate and silicate), dissolved organic nitrogen and phosphorus (DON and DOP), particulate organic matter (POM), in vitro incubation experiments such as ^{13}C and ^{14}C for primary production, community respiration and bacterial production, flow cytometry (bacteria and virus abundances, phytoplankton group abundances), eDNA, fatty acid, ^{15}N stable isotope and trophic transfer efficiency analyses, and phytoplankton and microzooplankton abundances.

CTD casts were taken using a hand-held self-logging CTD probe (CTD60M, Sea and Sun Technologies) equipped with additional sensors for oxygen and light PAR, every two days. This provided us with vertical profiles of temperature, salinity, pH, dissolved oxygen, chlorophyll a, and photosynthetically active radiation (PAR). Regarding sediment, every sampling day the mesocosm sediment traps were emptied, and their contents collected before general sampling began, using a vacuum system as described in Boxhammer et al. (2016).

3.1.2. Different Si:N ratios. (KOSMOSGC 2019)

In 2019 we conducted a mesocosm experiment which shows gradient in Si*. With Si* we mean the difference in concentration between Silicate and Nitrate. It has been reached by first manipulation of deep water, after the regular manipulation to get water similar to that at 700 meter-depth, and then by the addition to the mesocosm.

The experiment started on the first of September and ended on the 13th of October with a total duration of six weeks at Tailarte harbour, 35214 Telde, Las Palmas, Spain. The location is similar to that of the previous experiment, since we needed oligotrophic water to assess the effectiveness of artificial upwelling.

3.1.2.1. *Experimental set-up*

We utilized 8 mesocoms basically composed of a plastic bag with trap for sediment at the bottom and a cover in plexigrass. The plastic bag is about 2.5 meters length, of which about two meters in the water. All of them float and are anchored to the pier. Each mesocosm has in common the regular deep-water addition every 2 days. We created a gradient in Si* through the mesocosm. For Si* we mean $[Silicate] - [Nitrate]$. Thus, we obtained 2 groups of mesocosms: the first one with deep water addition containing more silicate than nitrate, the second one with more nitrate than silicate. How we can see in the picture below (Fig. 3.4) the lowest silica concentration treatments have deep water addition characterized by Si* values: -28, -20, -15, -10 µmol/l. The highest silica concentration treatments have deep water addition characterized by Si* values: -5, 0, +5, +10 µmol/l. This parameter was reproduced manipulating the deep-water in a different way for each mesocosms(treatment). On the right side, a summary of the target concentration of nitrates and silicates, to reach the Si* value listed above, with the N:Si ratio to better explain the parameter:

Nitrate (µmol/L)	Silicate (µmol/L)	N:Si
30	2	15:1
30	10	3:1
30	15	1
30	20	3:2
30	25	6:5
30	30	1:1
30	35	6:7
30	40	3:4

Figure 3.4. Schematic representation of mesocosm with corresponding Si* value.

Artificial upwelling simulation has been conducted, as in 2018, with an exchange of water between inside the mesocosm and deep water collected and manipulated. This was carried out by removing 4% of the volume of mesocosm water, and consequently adding the same amount of manipulated deep water.

A peristaltic pump was used for removing water from the mesocosm, which pumps water in pulses in order to maintain a constant flow rate of 14m³/h. It was important that the flow was constant in order to reduce the damage inflicted to organisms that were pumped out. Deep water was afterwards introduced using the dive pump and the “spider” (Fig. 3.6), nutrients were added manually with a canister into the same tube. It was also used to collect the deep water from the open ocean. In order to remove and put water homogeneously it has been utilized the same “spider” of previous KOSMOS 2018 experiment. The collection of deep water occurred four times during the experiments but unfortunately the collection deep water team didn’t reach the right depth thus after

collection the water has been manipulated to get water similar in nutrient concentration and ratio to that at 700 meters depth off the Canary Islands.

Figure 3.5. Photo of the eight mesocosms on the day before starting.

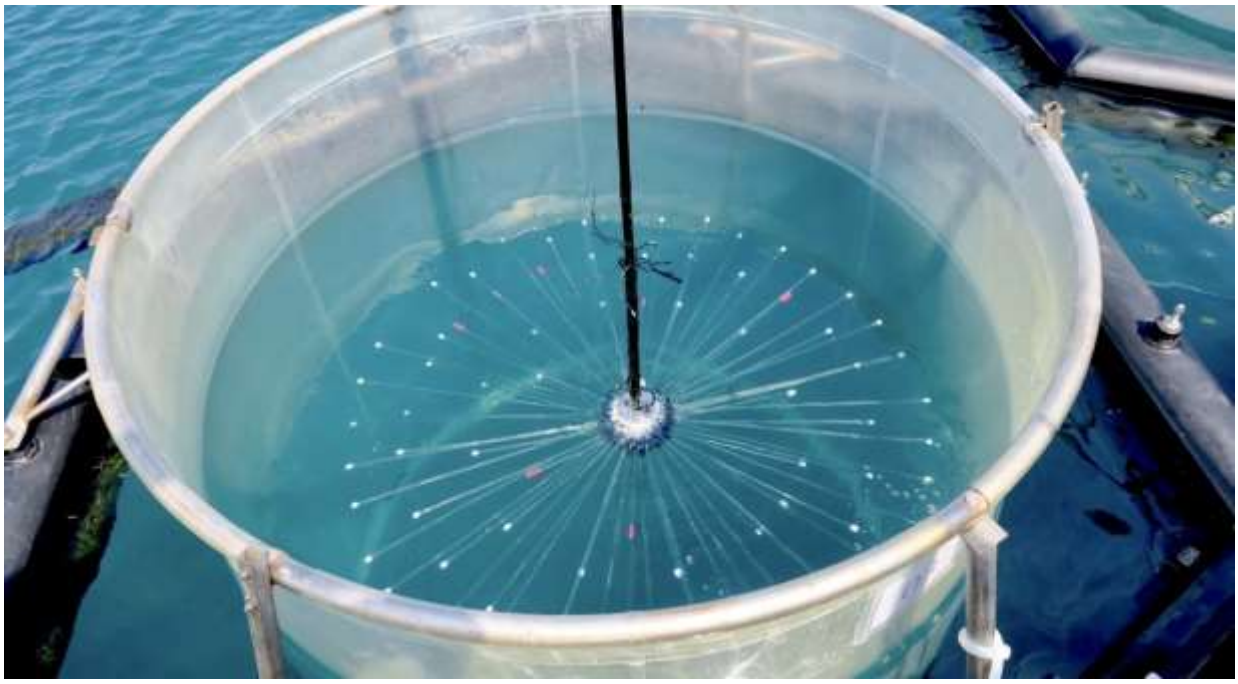

Figure 3.6. The spider.

3.1.2.2. Timeline

This experiment started on 6th of September and it ended on 11th of October. The duration of the experiment was 35 days in total, it began with the filling of the mesocosms

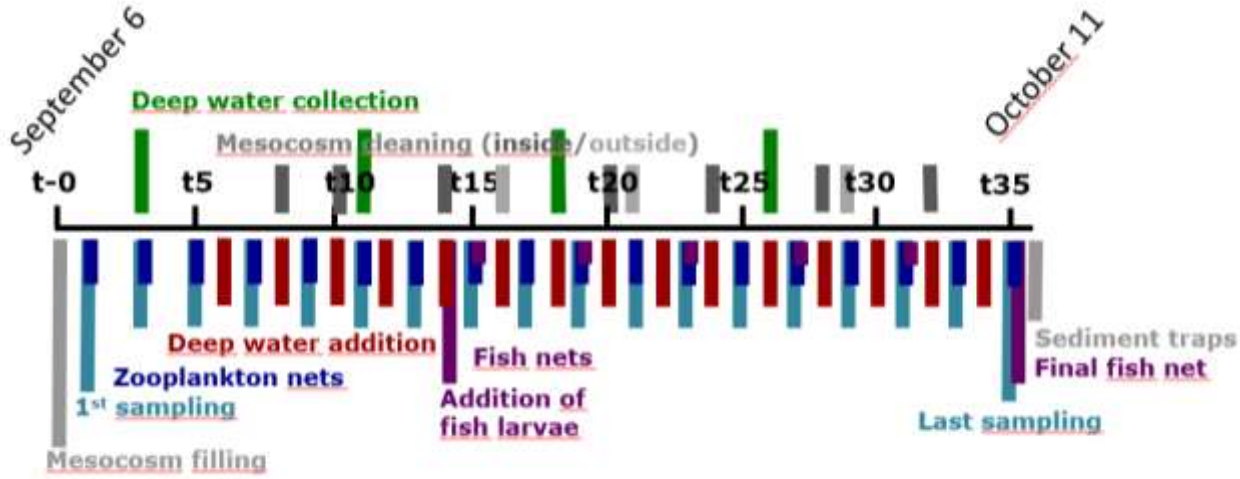

Figure 3.7. Schematic representation of the different activities carried out throughout the duration of the experiment. These include deep water collection (green), deep water addition (red), mesocosm filling (grey), regular sampling, which also includes sediment, and CTD casts (light blue), zooplankton net sampling (dark blue), fish larvae additions (purple), and final fishing of the whole mesocosm (purple), mesocosm cleaning (inside and outside)(two types of grey). Figure courtesy of Ulf Riebesell.

on t0 (September 6th) and ended with the last sampling and fishing of the mesocosms on t35 (October 11th).

3.1.2.3. Sampling

The sampling for the most physical, chemical and biological parameter took place every second day throughout the duration, some of them every fourth day. In particular sampling took place regularly from t1. (Figure 3.7).

The sampling was conducted by means of a sampler tube, consisting of a plastic tube with two openings, one at the bottom and one on the top. One opening ends with a small plastic tube useful for filling the sampling bottles. The tube can take in total about 5 L evenly from the mesocosm, given that it is as long as the mesocosms. After the filling of the tube, it is well mixed for 5 times.

Figure 3.8. Me while mixing the sampler tube. This figure shows the sampler tube and the mixing process.

The procedure followed has been described in Taucher et al. (2017) in order to sample for dissolved inorganic carbon (DIC), inorganic nutrients (nitrate and nitrite, ammonium, phosphate and silicate), dissolved organic nitrogen and phosphorus (DON and DOP), particulate organic matter (POM), in vitro incubation experiments such as ^{13}C and ^{14}C for primary production, community respiration and bacterial production, flow cytometry (bacteria and virus abundances, phytoplankton group abundances), eDNA, fatty acid, ^{15}N and ^{14}C stable isotopes for trophic transfer efficiency analyses, and phytoplankton and microzooplankton abundances. The most of these, as CTD analysis are common to the previous experiment. For sediment we used the vacuum system described in Boxhammer et al. (2016).

3.1.3. Biogeochemical analysis

In order to answer to the scientific questions, we need to carry out some biogeochemical analysis. In particular, they are the determination of: Chlorophyll α, particulate organic carbon (POC), carbon uptake using stable isotopes, nitrogen in its forms, dissolved silica, biogenic silica, silica uptake and phytoplankton taxonomic identification.

3.1.3.1. *Sampling for biogeochemical analysis*

The sampling was a part of the general sampling, thus it was carried out every second day for the most parameters instead for silica uptake with PDMPO method, it took place three times during the experiment. The sampling consists in taking out water from the mesocosm with the sampler tube. It follows a mix of that to make it homogeneous and the filling of the respective bottles for the subsequent analysis.

3.1.3.2. *General phytoplanktonic biomass and productivity measurements*

In both these experiments, phytoplankton biomass and its productivity were taken into account. Phytoplankton biomass is determined using chlorophyll α and POC as proxies, while regarding productivity was measured using stable isotopes of nitrogen and carbon. The first one consists in the measuring of the quantity of phytoplankton in the seawater. This determination includes extraction of chlorophyll α, after filtration, with 90 % acetone. It follows the absorption of the extracted chlorophyll and the measure with the spectrophotometer and its concentration calculated. (after Jeffrey & Humphrey 1975).

The POC measure consists in a first filtration of the samples through combusted GF/F filters. It follows the removal of inorganic carbon by hydrochloric acid. Subsequently a drying is needed. The determination is made as describe by Sharp, J.H. 1974. The data about chlorophyll α, POC and about productivity from stable isotopes will not include in this thesis.

Microscopy analysis for taxonomy identification has been carried out for the entire duration of the experiment, every two days. It has been conducted with the analysis of the sampled water with macroscopy identification to identify the taxonomic groups considering also abundance inside the group. It was necessary to understand the development of phytoplankton community during the experiment.

3.1.3.3. Forms of Nitrogen

The various nitrogen forms were measured using the method written by Sharp, J.H. 1974. They are not included in this thesis.

3.1.3.4. Inorganic silica

For the aim of this study all form of silica are considered important and measured, in particular inorganic silica, also called dissolved silica, is determined by addition to the 10ml of sample of the mixed reagent with MoO_4^{3-} then a mixing is required. It follows, after 10-20 minutes, the addition of 0.2 ml oxalic acid and then immediately 0.2 ml ascorbic acid. The measure is carried out, after 30 minutes by determining the absorption at 810 nm in 1 cm cuvettes against artificial sea water. Here the precision is:

- ✓ low values (4.5 µmol/ l $Si(OH)_4$-Si) ± 4 %
- ✓ intermediate values (45 µmol l^{-1} $Si(OH)_4$-Si) ± 2.5 %
- ✓ high values (100 µmol/ $Si(OH)_4$-Si) ± 6 %

3.1.3.5. Biogenic silica

Biogenic silica is quantified with the method proposed by (Grasshoff K., K. Kremling and M. Ehrhardt (1999)) by which the particulate biogenic silicate is converted to dissolved silicate by leaching with 0,1M NaOH at 85°C. It follows the same procedure for dissolved silica.

All the data included in this thesis are preliminary, thus the errors in general calculated from the standard deviation, are not included.

3.1.3.6. Silica uptake

The silica uptake can be measured with some methods. I utilized the PDMPO method. This is made up of one qualitative and one quantitative analysis. This method is based on the use of the fluorescent dye, 2-(4-pyridyl)-5-((4-(2-dimethylaminoethylaminocarbamoyl)methoxy)phenyl)oxazole also called PDMPO. PDMPO was synthesized for the first time by Diwu et al. (1999) not for this purpose but for being a pH indicator for acidic cellular organelles. Subsequently, it has been found by Shimizu et al. (2001) that PDMPO was incorporated into silica deposition vesicles and, in particular, that PDMPO goes into newly formed diatom frustules. In addition to that, its fluorescent intensity tends to increase when silicification occurred in the presence of silicic acid. (Shimizu et al. 2001). Moreover, PDMPO can be a useful dye to quantify the silica uptake since it is incorporated in a ≈ nearly constant ratio with biogenic silica. It follows

that the silicification rate of the total diatom community can be quantitatively determined by applying the bSiO2:PDMPO ratio to the amount of PDMPO incorporated (LeBlanc and Hutchins 2005). However, still now the measure of biogenic silica production cannot be quantitatively determined in single cells by PDMPO incorporation. It can be only qualitative by using the ultraviolet microscope.

The method wrote by McNair, H.M., Brzezinski, M.A., Krause, J.W. (2015), with the aim of “Quantifying diatom silicification with the fluorescent dye, PDMPO”, includes sampling, incubation, measurement and calculation. In the first step, the sampling is prepared through filling three bottles for each mesocosm, two will contain the PDMPO dye, called treatments, and one will not contain it, called blank. Each bottle can contain a volume around 310 ml. It follows the thawing and centrifugation of vials of PDMPO, one for each treatment bottle. Each vial contains 50µl of PDMPO, figure 3.9. The incubation starts after the addition of 48 µl of PDMPO in each treatment bottle, properly labelled, and incubating them for 24h. The incubation occurred at the fountain of “Parque Tecnológico”, because it mimics natural conditions of the mesocosm. The measurement includes the filtration onto polycarbonate filters (1.2 lm pore, 25 mm diameter). Before filtration, 50 mL aliquot of one of the bottles with PDMPO inside, for each mesocosm, was removed and stored for taking note of the subsequent, qualitative, single cell PDMPO incorporation. The filters are transferred to a 15 mL polypropylene conical centrifuge tube, covered in 10 mL of 100% methanol. They were stored in a fridge at 4°C until they could be measured (often after days), even if in the right protocol state that they must be kept in the fridge for 24 hours. Afterwards, in order to put the filters to the bottom of the tube to suck methanol supernatant to 1mL, they have been centrifugated (10 min, 1230 3 g) to pellet the cells and we tried to use the Teflon rod as written in the protocol however the surnatant tended to go out thus we took out methanol using a pipette. The tube with the filters inside were dried in a vacuum oven at temperature < 60°C. The dried frustule-bound PDMPO need to be solubilized and quantified by using fluorometer. This was carried out adding 0.2 mL of 0.5M HF, mixed it with Teflon rod in order to remove air

Figure 3.9. The PDMPO vial.

bubbles from the filter to allow contact between cells and the HF. The samples were left to a 1-h digestion, then they were neutralized with 2.8 mL of saturated boric acid (1 M). It follows the measurement of fluorescence of the solution using “a Trilogy Laboratory Fluorometer (Turner designs) with the crude oil snap-in module (Light Emitting Diode (Center Wavelength) 365 nm, excitation 350/80 nm, emission 410–600 nm)”. The value of raw fluorescence will be converted to PDMPO concentration using a standard curve of known concentrations of PDMPO. Now the PDMPO concentration has to be converted into biogenic SiO2. This will be made using results from this article (McNair, H.M., Brzezinski, M.A., Krause, J.W. , 2015), they found the mole ratio of the increase in biogenic silica to the incorporation of PDMPO (bSiO2 : PDMPO) for eight species with a median value of 2916±6708 (SE), n58.

3.2. Data analysis

3.2.1. Silica uptake

To assess indirectly the silica uptake it has been also used data of dissolved silica, the molarity of silicon in deep water added and its volume. It has been calculated first with a silica budget:

In 2018

$$M_{(\mathrm{ada})} = {(M_{(\mathrm{bda})} * 35000 - M_{(\mathrm{bda})} * WEV + M_{(\mathrm{dp})} * \ \mathrm{WEV})}/{35000}$$

Where with $M_{(ada)}$ I mean the molarity right after the deep-water addition, with $M_{(bda)}$ the molarity before the deep-water addition, with 35000 liter the volume of each mesocosm and with WEV the water exchanged volume.

In 2019

$$M_{(\mathrm{ada})} = {(M_{(\mathrm{bda})} * MV - M_{(\mathrm{bda})} * WEV + M_{(\mathrm{dp})} * \ \mathrm{WEV} + \mathrm{Si\ added})}/{MV}$$

Where with $M_{(ada)}$ I mean the molarity right after the deep-water addition, with $M_{(bda)}$ the molarity before the deep water addition, with WEV the water exchanged volume and with MV the mesocosm volume.

Second, I calculated for both experiment the silica uptake as:

$$Silica\ uptake = (M(Si)after\ deep\ water\ addition - M(Si)before\ next\ deep\ water\ addition)/\Delta time$$

3.2.2. Biogenic silica/Diatoms abundance ratio

This indicator has been thought as the average quantity of biogenic silica in µmol/L contained in each cell of diatoms. This could be used as a proxy for the thickness of the diatom wall cell.

The visualization of the graphs was done using the R software, version 1.2.1335

3.2.3. Statistics

During data analysis some statistics were carried out. In particular correlation between dissolved and biogenic silica to understand the relation between them before and after the deep-water addition and also to understand indirectly the silica uptake.
More correlations include biogenic silica and diatom abundance, both integrated throughout the experimental duration, to understand the effect of the treatments on the quantity of biogenic silica per cell. It has been used α=0.05 in order to evaluate the significance inside the correlations. The p value taken is obtain by permutation. The correlations were carried out with PAST, version 3.26.
To highlight the consequences of silica uptake in developing of diatom community in these two experiments, PCAs were carried out. In 2018 experiments all the variables included were transformed by the function $log(V + 1)$, it follows a normalization with the function $(x - mean)/stdev$, where V stand for variable and x for transformed variable. The variables included are chlorophyll-a, bSi, dSi, diatom abundance, chlorophyll-a/biogenic silica ratio and biogenic silica/diatom abundance. It has been made with these features in total 3 PCA, one for Pulsed treatments with control, one for Continuous treatments with control and then one with all of them.

In 2019 experiments the PCA has been made before (day 5) and after (day 9) the first deep-water addition and one for the entire period of the experiment. In this PCA it has been decided to include these variables: dissolved silica, chlorophyll α, biogenic

silica/diatom abundance, chlorophyllα/biogenic silica and diatom abundance, while biogenic silica has been excluded because highly correlated with diatom abundance (r^2= 0.70475 an p= 0.0001). Here the principal component analysis has been made with previous transformation of three variables with the function $log(V + 1)$, they were: diatom abundance and biogenic silica/diatom abundance. It follows the normalization with $\frac{(x-mean)}{stdev}$ to make the PCA. The Eigenvalues and the Eigenvectors are showed in the appendix 1.

4. Results

4.1. Dissolved silica

These two graphs (Fig. 4.1 and 4.2) show the trend of dissolved silica, where it can be noted the peak corresponding to the addition of deep water and a rapid decline due to the uptake by diatoms. In both figures (4.1 and 2) it is nicely possible to see only a big peak in dissolved silica, due to the first deep water addition. In the first experiment (Fig. 4.1) the peak is at around 5µmol/L for the mesocosm with 49% of deep-water addition, then we have some increasing in dissolved silica after each addition in continuous mode. The other values are close to zero. In the end, an increasing occurs for the continuous treatment with the highest percentage of added deep water. The control shows a constant value close to zero.

In the second experiment (Fig.4. 2), after the first peak, all mesocosm values are close each other and very close to zero, except for some small peak around day 19, 21 and 29.

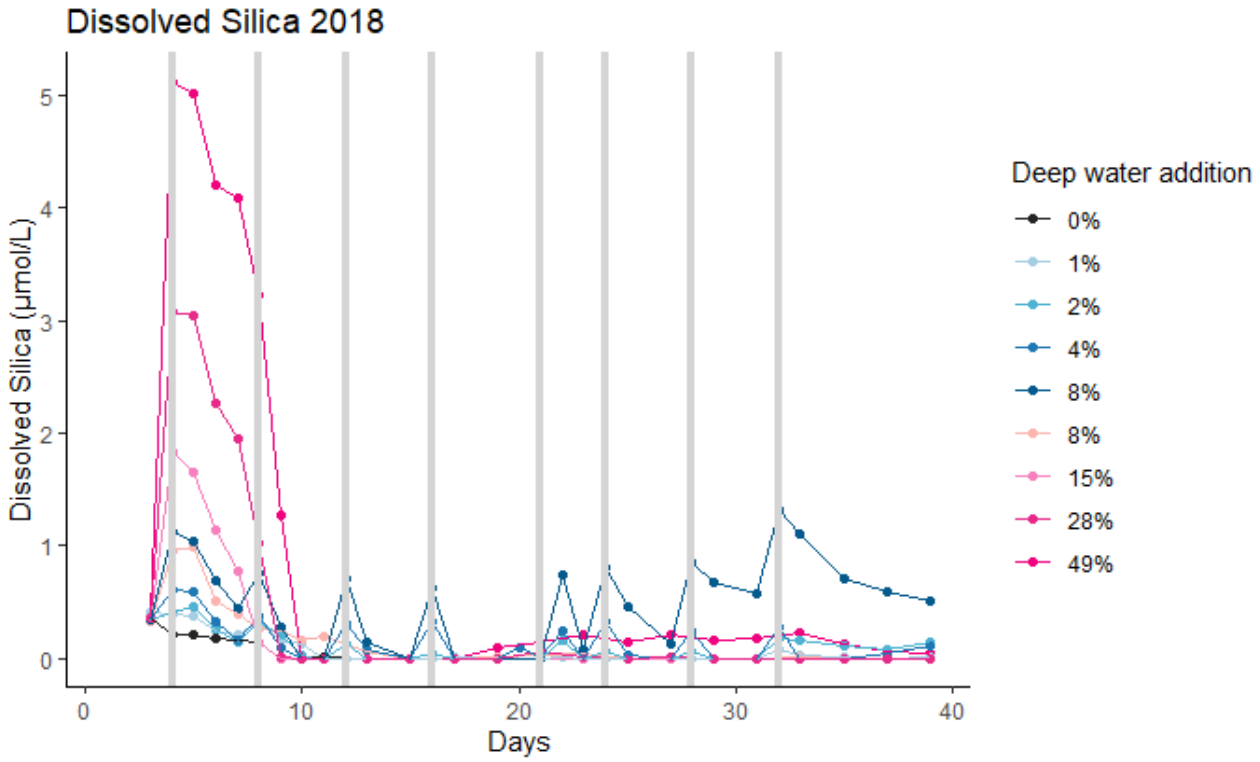

Figure 4.1. Temporal development of dissolved inorganic silica during the 2018 experiment. Black stands for the control in which no deep water was added, blue colours correspond to continuous treatments and pink for pulsed treatments. The grey bars in the background signal the deep-water addition events on date 4 the pulsed treatments and days 4, 8, 12, 16, 20, 24, 28 and 32 for the continuous treatments. The legend shows the percentage of water in each mesocosm that was substituted by nutrient-rich deep water per addition.

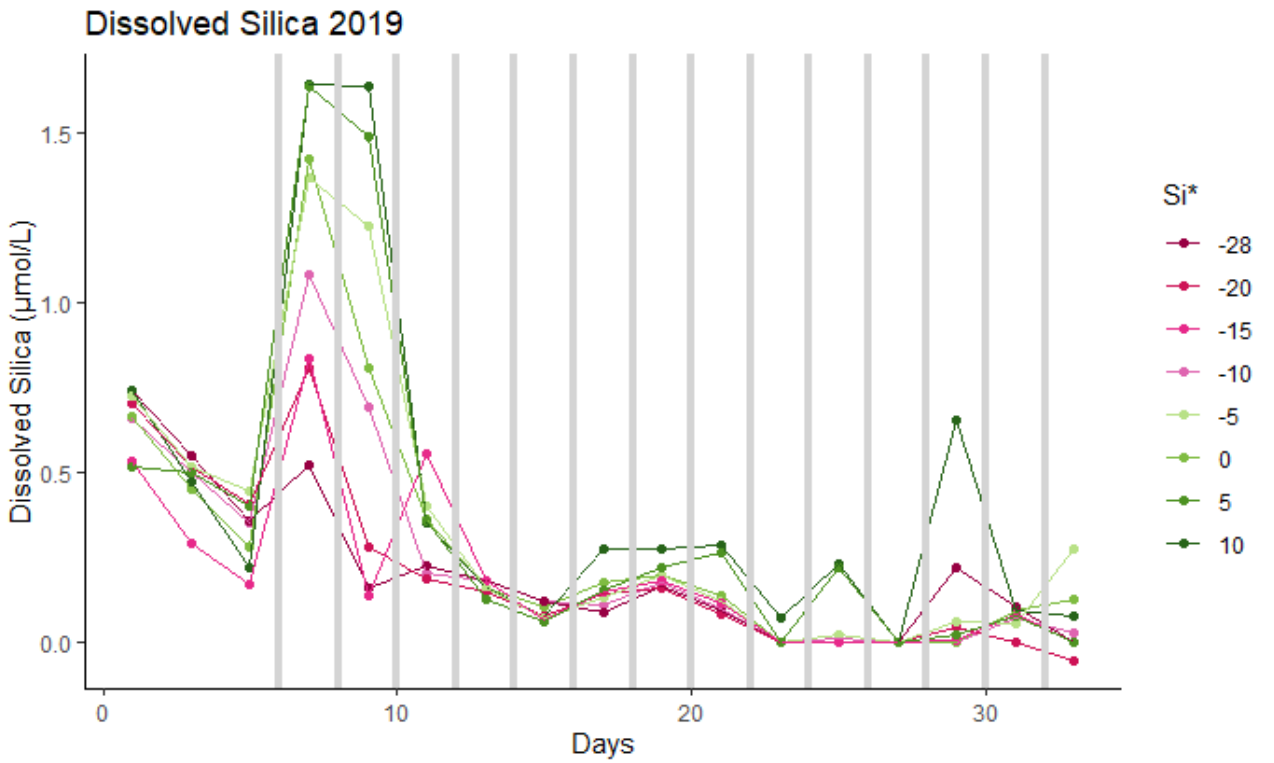

Figure 4.2. Temporal development of dissolved inorganic silica during the 2019 experiment. Pink colours correspond to low Si* treatments and green for high Si* treatments. The grey bars in the background signal the deep-water addition events on days 6, 8, 10, 12, 14, 16, 18, 20, 22, 24, 26, 28, 30 and. The legend shows the value of Si* of the deep water added every two days.

4.2. Biogenic silica

The biogenic silica appears and increases after deep-water addition with high Si:N ratio.

Biogenic silica (bSi) recorded in 2018 experiment (Fig. 4.3) shows two different trends: pulsed treatments show a peak around day 9 and then a decreasing trend. The highest value in pulsed treatment is over 3 µM. In continuous treatments, an increasing in bSi value is found until day 31. In the mesocosm with 8% of deep-water addition, a peak around day 17 has been found, with a biogenic silica value over 2µM, followed by a decline. The control shows a constant value close to zero.

In 2019 experiment, two trends can be found (Fig. 4.4). One with high Si* values and one with low Si* values. In the first one we have a continuous increasing trend in biogenic silica values, while in the second one we have a constant trend or a slight increase, in particular in the mesocosms with Si* values of -15 and -20. The mesocosm with Si* value of -28 shows a slightly decreasing trend, while the one with Si* value of -10 shows an increasing trend.

The term Si* stands for the difference in concentration between Silicate and Nitrate.

$Si^* = [Silicate] - [Nitrate]$

Taking into account both experiments, the biogenic silica production is influenced by the quantity of water exchanged and also by the N:Si ratio. More consequences and conclusions can be found in the next chapter.

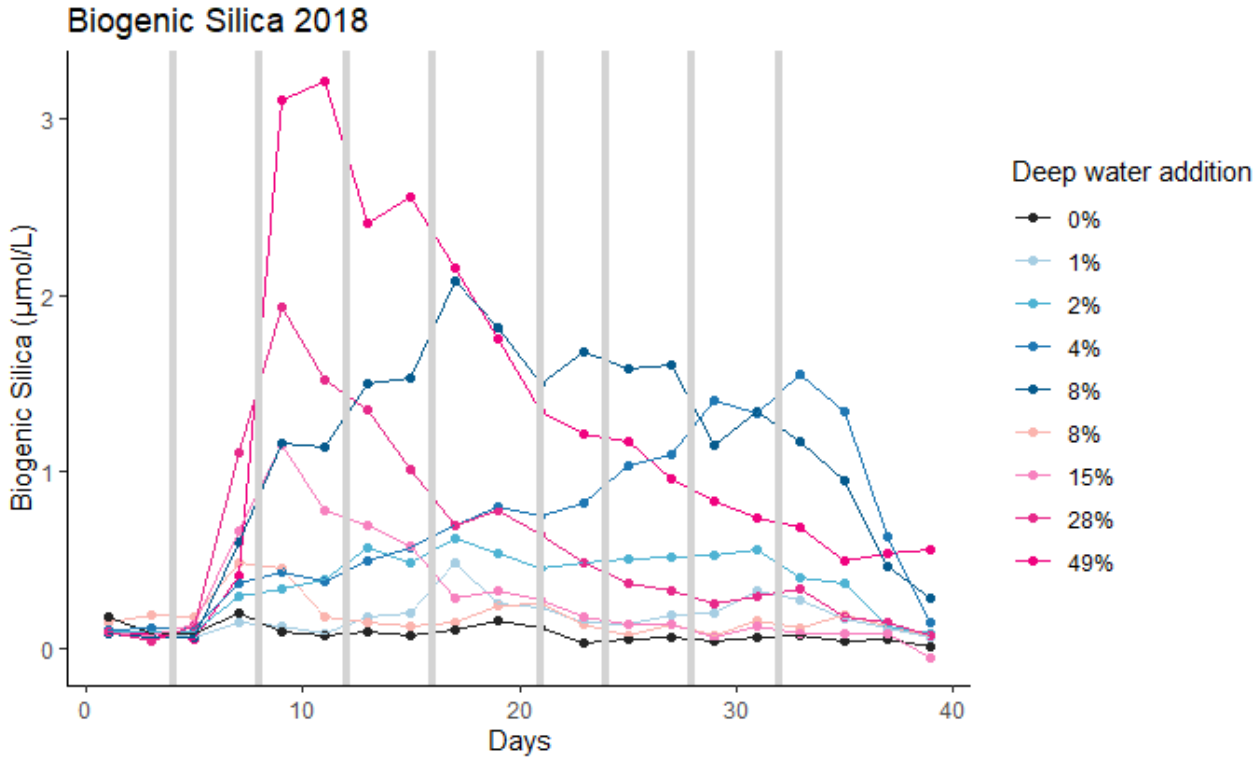

Figure 4.3. Temporal development of biogenic silica during the 2018 experiment. Black stands for the control in which no deep water was added, blue colours correspond to continuous treatments and pink for pulsed treatments. The grey bars in the background signal the deep-water addition events on date 4 the pulsed treatments and days 4, 8, 12, 16, 20, 24, 28 and 32 for the continuous treatments. The legend shows the percentage of water in each mesocosm that was substituted by nutrient-rich deep water per addition.

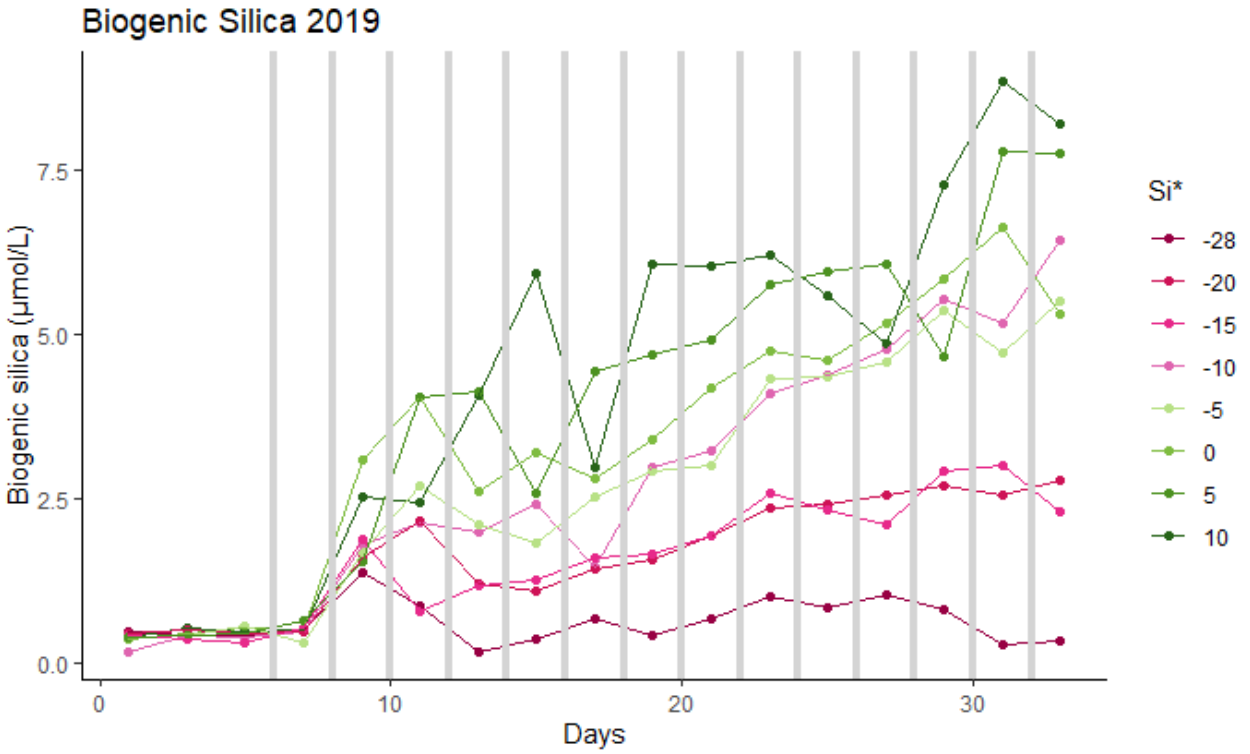

Figure 4.4: Temporal development of biogenic silica during the 2019 experiment. Pink colours correspond to low Si* treatments and green for high Si* treatments. The grey bars in the background signal the deep-water addition events on days 6, 8, 10, 12, 14, 16, 18, 20, 22, 24, 26, 28, 30 and. The legend shows the value of Si* of the deep water added every two days.

4.3. Diatom abundance

Diatom abundance increases with deep-water addition, since it represents the ecological response of deep-water addition. The abundance of diatoms in 2018 experiment (Fig. 4.5) shows a peak around day 9 for pulsed treatments and later for continuous treatments. Most continuous treatments show an increasing trend followed by a decline. In particular, the ones with 2%, 4% and 8% of deep water exchanged every 4 days (continuous mode), show this trend, while the one with 1% of deep water exchanged (continuous mode) shows a constant value just above zero. The control shows a constant value close to zero during the entire duration of the experiment, except for a small peak on the day 9.

In 2019 experiment (Fig. 4.6) we found a continuous increase of diatom abundance in all mesocosms, with overlapping of the most mesocosms. Only the one with the lowest value in Si* tends to decrease in the beginning. A completely different trend has been found in the one with the highest value in Si*(Si*=10), where we found a peak in the middle of the experiment.

Moreover, the difference in composition and in abundance of diatoms between the highest and the lowest silica treatment can be appreciated by looking microscope photos taken from the microscope team. The photos of the day 19 for the highest and the lowest treatment are shown below. In the one of the lowest Si* treatment (Si*=-28) (Fig. 4.7) low abundance of diatom can be noticed.

In one of the highest Si* treatment (Si*=10) (Fig. 4.8) high abundance can be appreciated. From these microscope photos, differences in composition can be noticed too, but, here, in this thesis the diatom composition has been not taken into account.

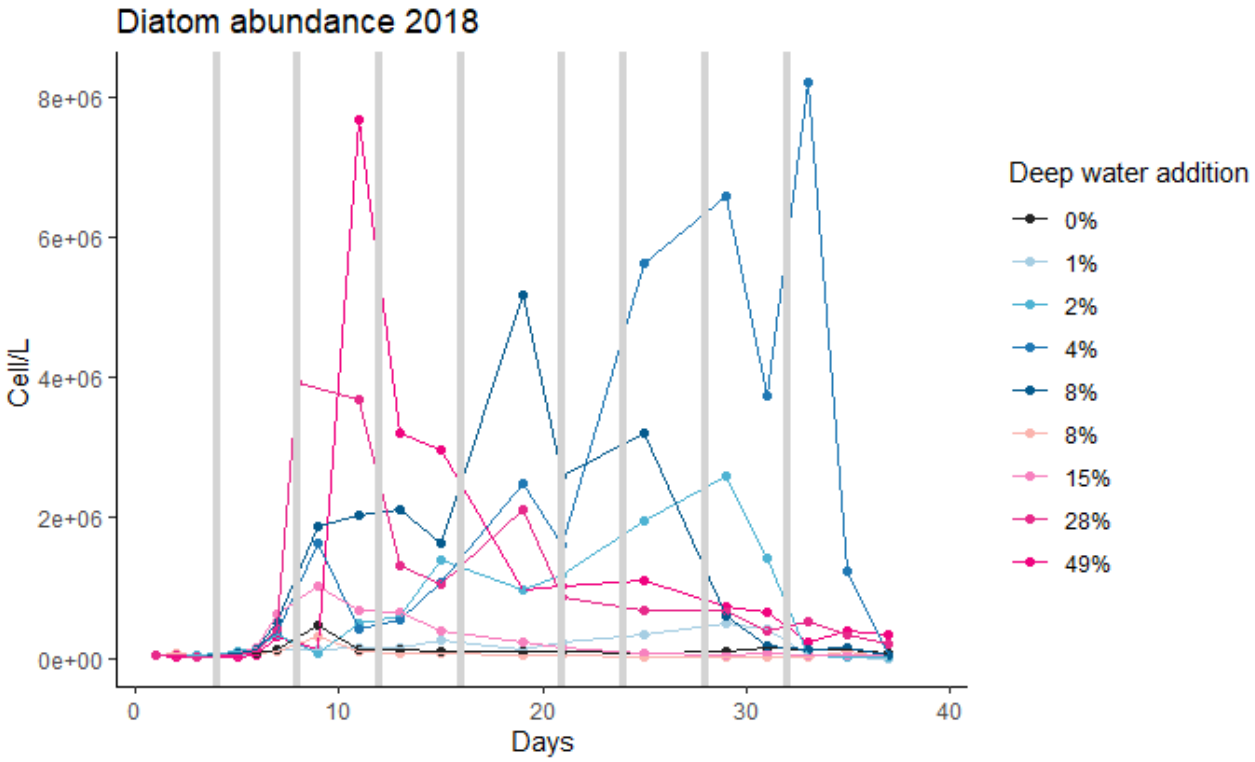

Figure 4.5. Temporal development of diatom abundance during the 2018 experiment. Black stands for the control in which no deep water was added, blue colours correspond to continuous treatments and pink for pulsed treatments. The grey bars in the background signal the deep-water addition events on date 4 the pulsed treatments and days 4, 8, 12, 16, 20, 24, 28 and 32 for the continuous treatments. The legend shows the percentage of water in each mesocosm that was substituted by nutrient-rich deep water per addition.

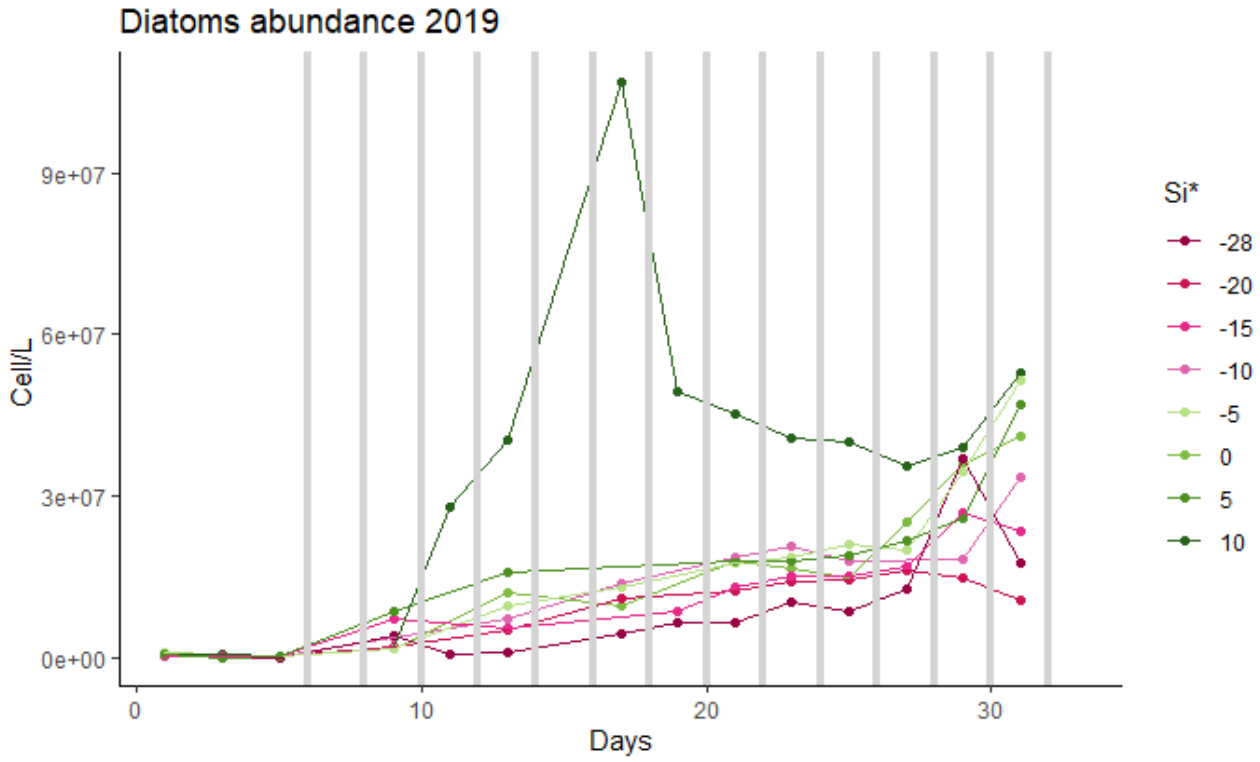

Figure. 4.6. Temporal development of diatom abundance during the 2019 experiment. Pink colours correspond to low Si* treatments and green for high Si* treatments. The grey bars in the background signal the deep-water addition events on days 6, 8, 10, 12, 14, 16, 18, 20, 22, 24, 26, 28, 30 and. The legend shows the value of Si* of the deep water added every two days.

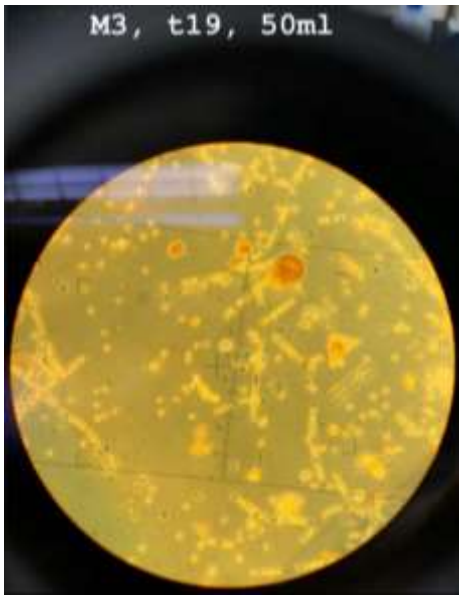

Figure 4.7. Photography on the microscopy for mesocosmos with Si*=-28 on the 19th day, of the 2019 experiment.

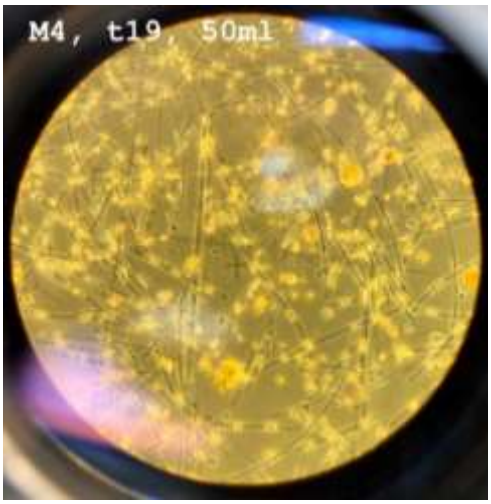

Figure 4.8. Photography on the microscopy for mesocosmos with Si*=10 on the 19th day, of the 2019 experiment.

4.4. Silica Uptake

The silica uptake graph of 2018 experiment (Fig. 4.9) is quite different respect the one of 2019 experiment (Fig. 4.15).

4.4.1. 2018 experiment

In the first experiment (Fig. 4.9) diatoms take up silica, for the most, in the first part of the experiment in pulsed treatments, while in continuous treatments they show pretty constant values over time, as expected we have an increasing along the percentage of deep water added.

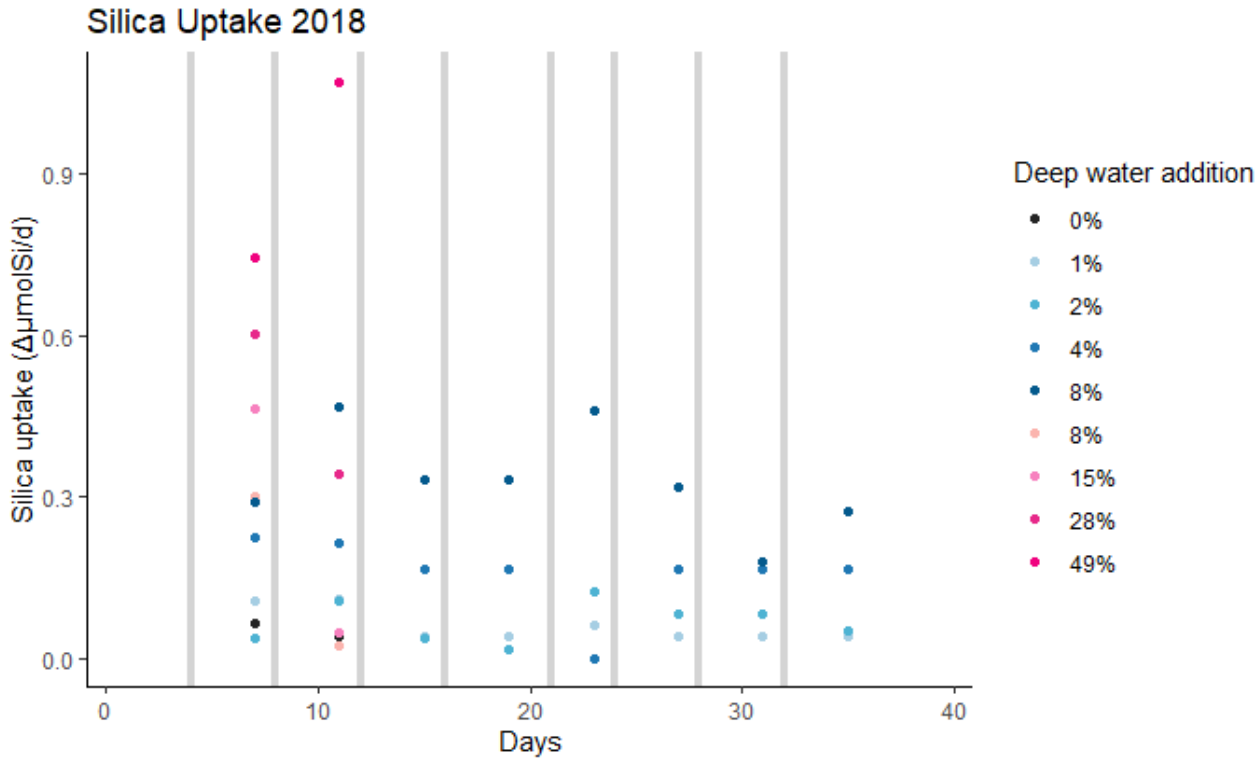

Figure 4.9. Temporal development of silica uptake during the 2018 experiment. Black stands for the control in which no deep water was added, blue colours correspond to continuous treatments and pink for pulsed treatments. The grey bars in the background signal the deep-water addition events on date 4 the pulsed treatments and days 4, 8, 12, 16, 20, 24, 28 and 32 for the continuous treatments. The legend shows the percentage of water in each mesocosm that was substituted by nutrient-rich deep water per addition.

It will be displayed better in the next three figures the uptake of silicate plotting biogenic silica to dissolved silica for the days 3rd (Fig. 4.10), 5th (Fig. 4.11 and 4.12) and 7th (Fig. 4.13 and 4.14) for the 2018 experiment. It is possible to see a pretty constant value right before the first addition of deep water, on the day 3 (Fig. 4.10), while right after it, at days 5th (Fig. 4.11 and 4.12) and 7th (Fig. 4.13 and 4.14), it can be possible to observe an increasing in bSi value respect the dSi value, with the increasing in deep water addition. Moreover, this curve tends to reach a plateau on the 7th day (Fig. 4.14), the day that coincides with the beginning of the peak in biogenic silica. This means that diatoms uptake silicate with an upper limit.

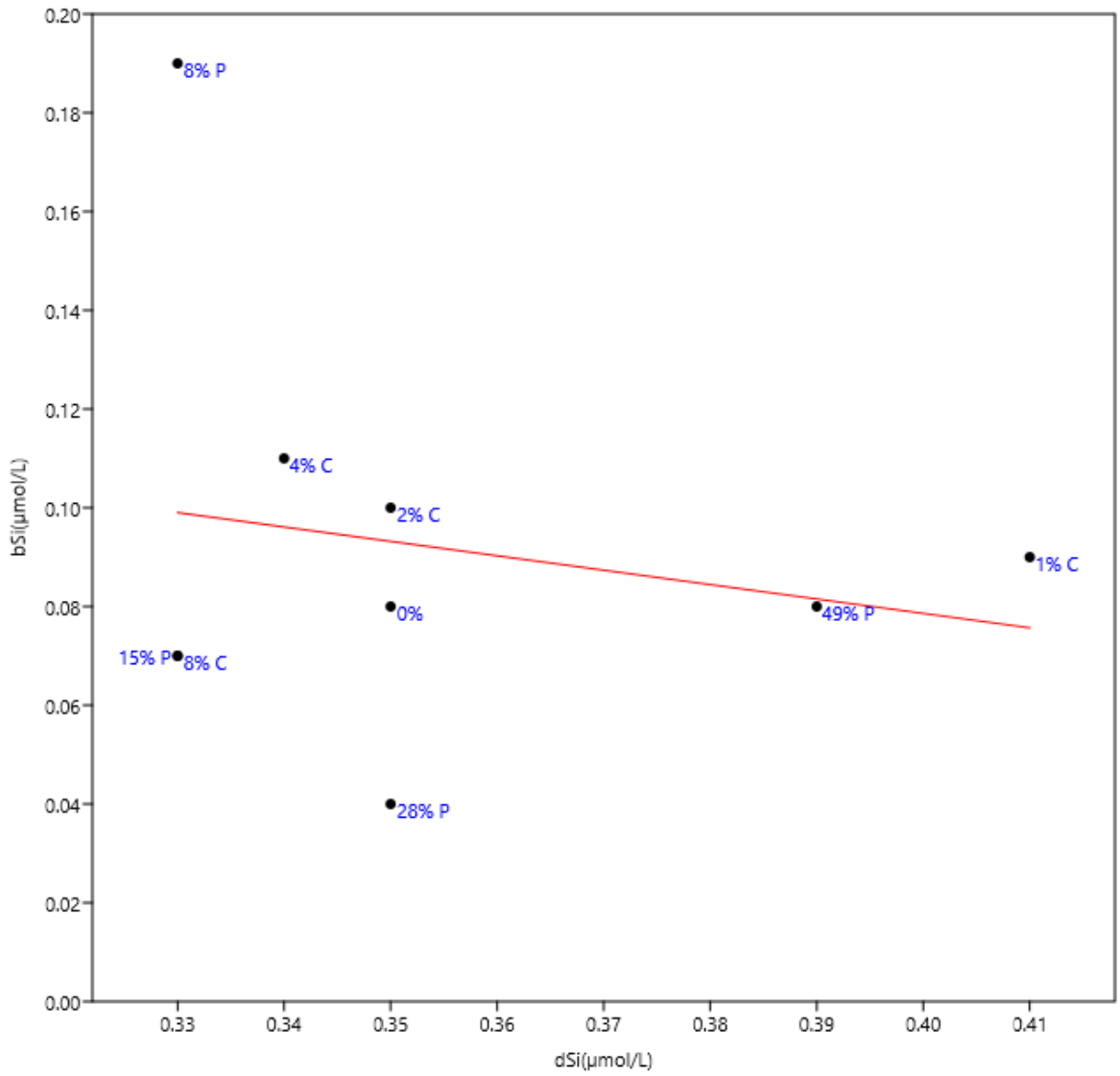

Figure 4.10. Correlation between biogenic silica and dissolved silica on the 3rd day of the experiment in 2018.

Specifically, in the third day the correlation curve is given by the equation $bSi = -0{,}29167 dSi + 0{,}19528 \mu mol/L$ with r^2= 0,039013 and p= 0,580, thus not significant.

The data on the 5th day shows two patterns: with and without the value corresponding to 49% of deep water exchanged. Thus, they both are shown. The first one is shown below. Here (Fig. 4.11), the equation is $bSi = -0{,}0057078dSi + 0{,}10959\mu mol/L$ with r^2= 0,048559 and p value of 0,557, thus not significant.

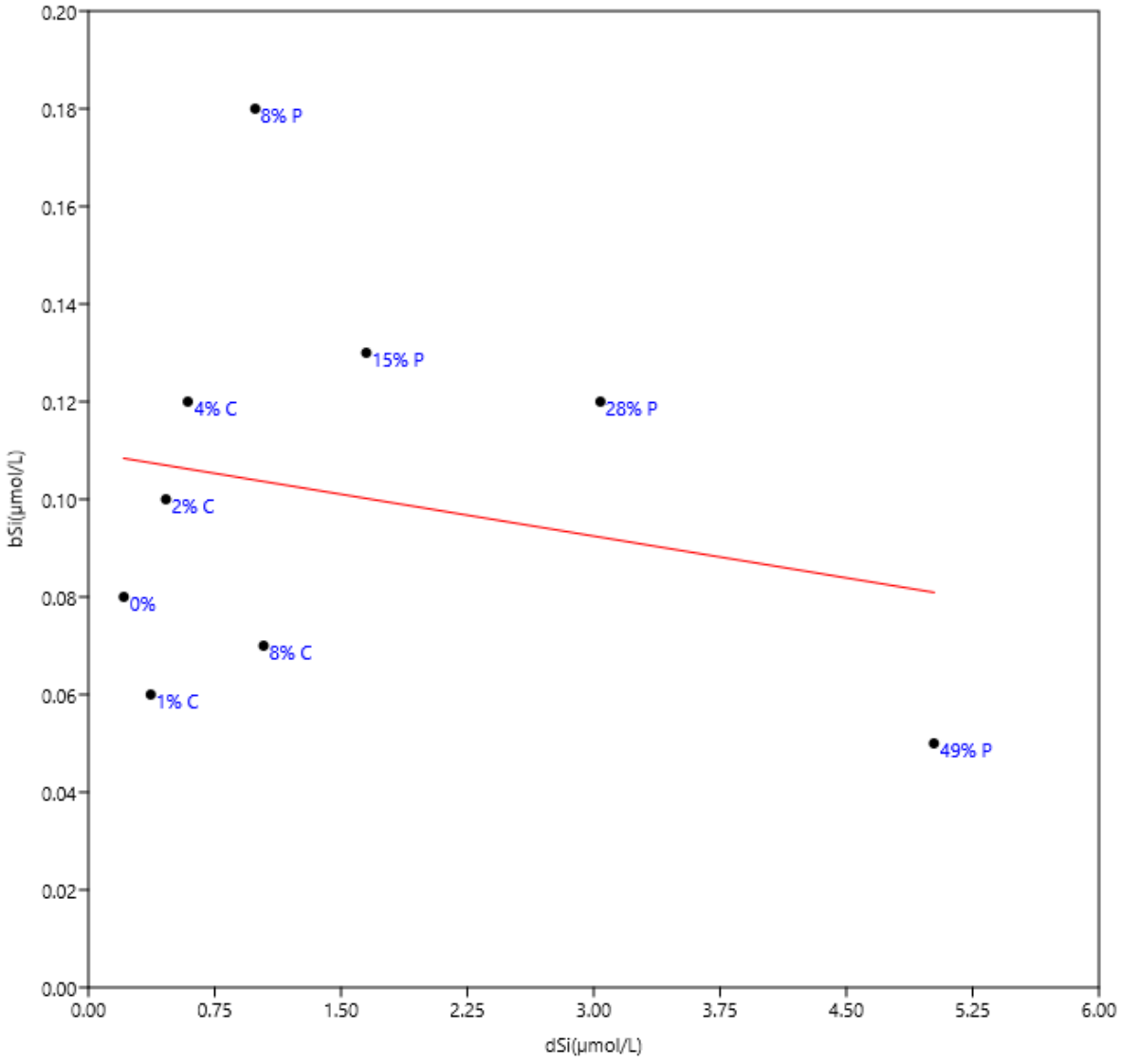

Figure 4.11. Correlation between biogenic silica and dissolved silica on the 5th day of the experiment in 2018.

The correlation between biogenic silica and dissolved silica on the 5th day, without data of the mesocosm with 49% of water exchanged, is shown below (Fig. 4.12). There the equation is $bSi =$ 0,014621dSi+0,092239µmol/L, r^2= 0,12262 and p= 0,401, not significant.

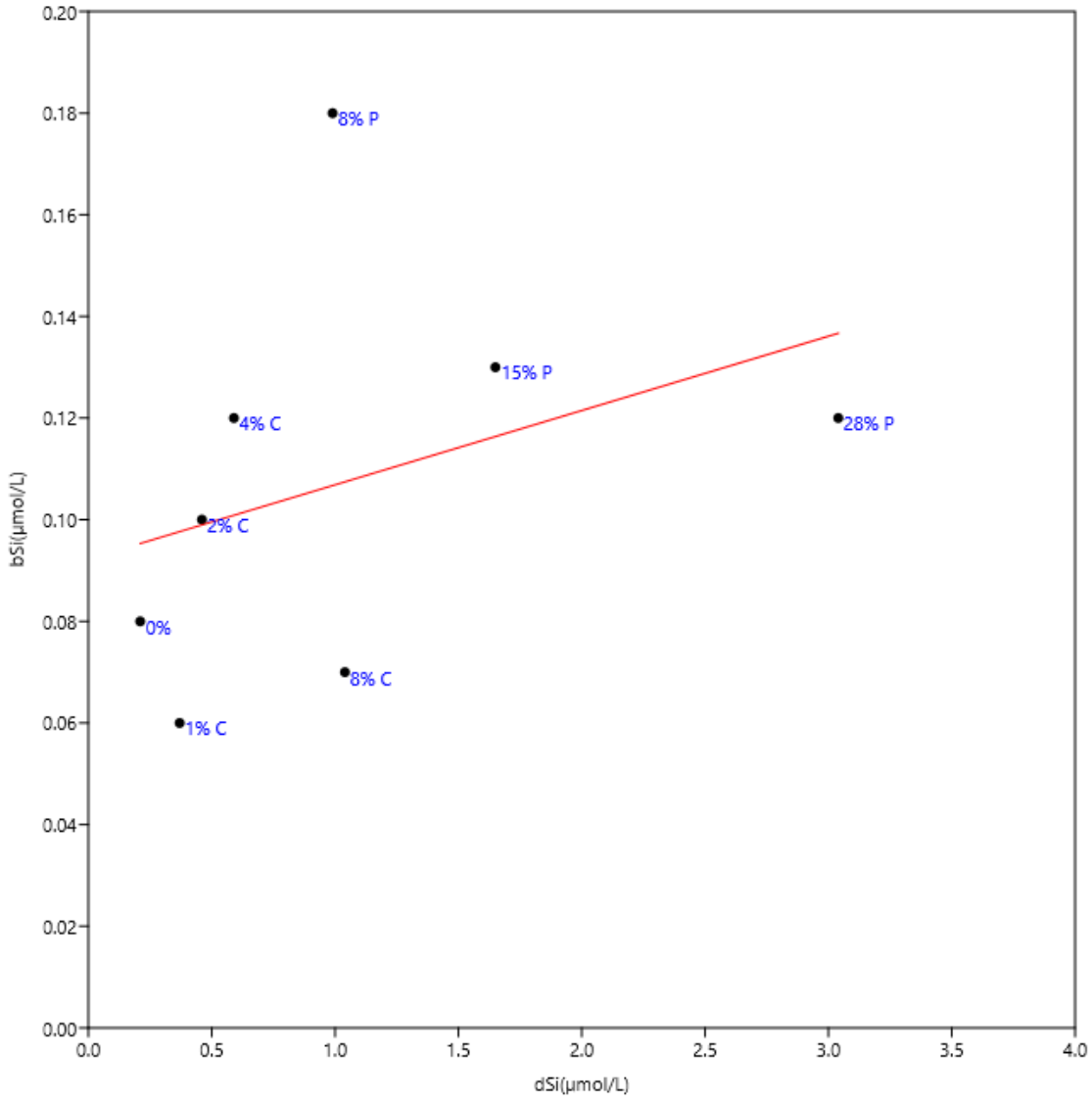

Figure 4.12. Correlation between biogenic silica and dissolved silica on the 5th day of the experiment in 2018.

On the 7th day the trend seems to be not so linear, for this reason only two figures, one with linear correlation (Fig. 4.13) and one with power correlation (Fig. 4.14) are shown below. In the plot with linear correlation (Fig. 4.13) the equation is $bSi = 0{,}073954dSi + 0{,}4053$ with r^2=0,11051 and p= 0,321, thus not significant. In the plot with power correlation (Fig. 4.14) the equation is $bSi = 656{,}03dSi^{0{,}00023148} - 655{,}43$µmol/L. On the 7th day it is clearer that phytoplankton community incorporate dissolved silica into biogenic

silica until reaching a plateau while the addition in the amount of 49% exceeds the capacity of utilization.

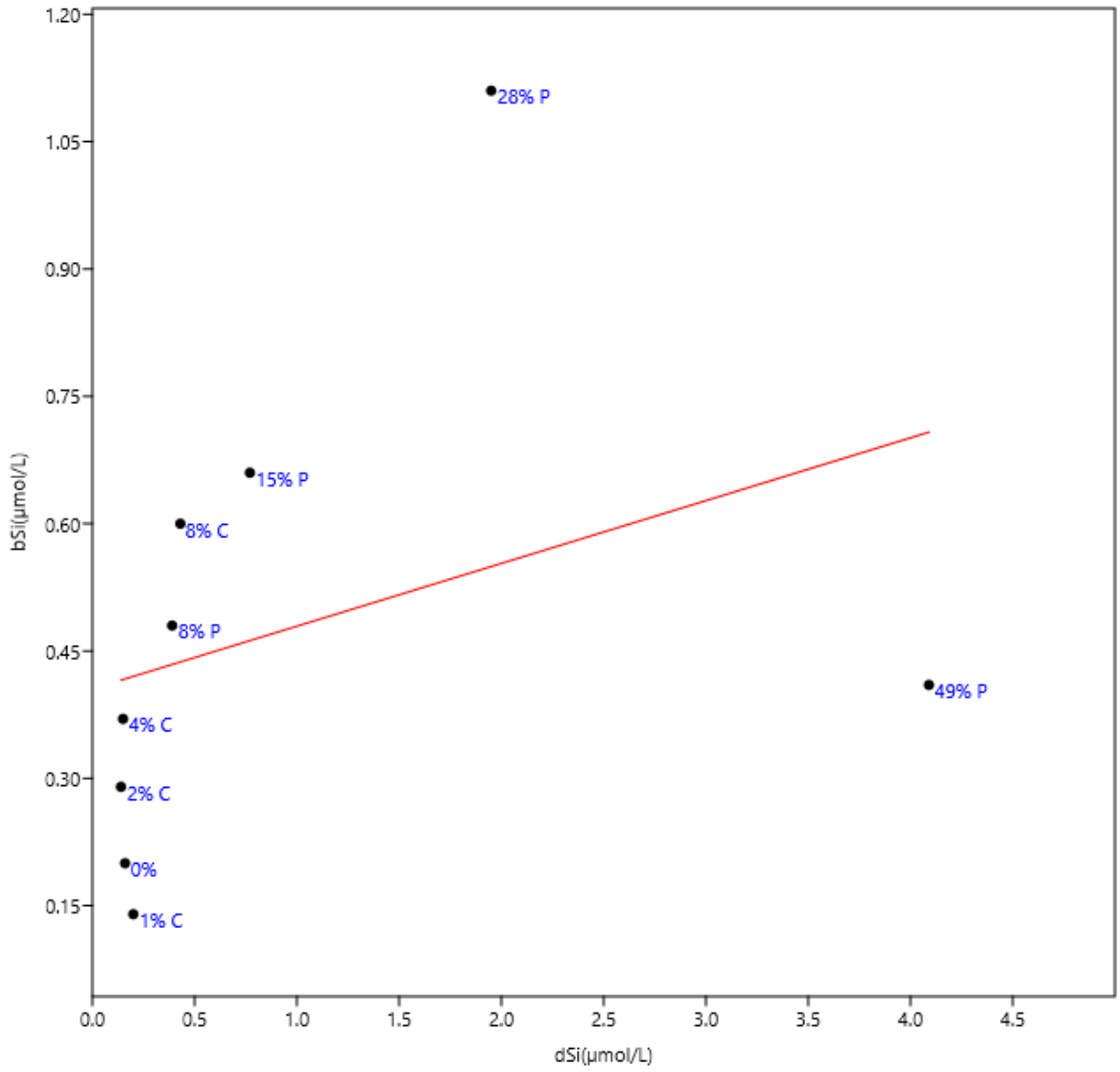

Figure 4.13. Correlation between biogenic silica and dissolved silica on the 7th day of the experiment in 2018.

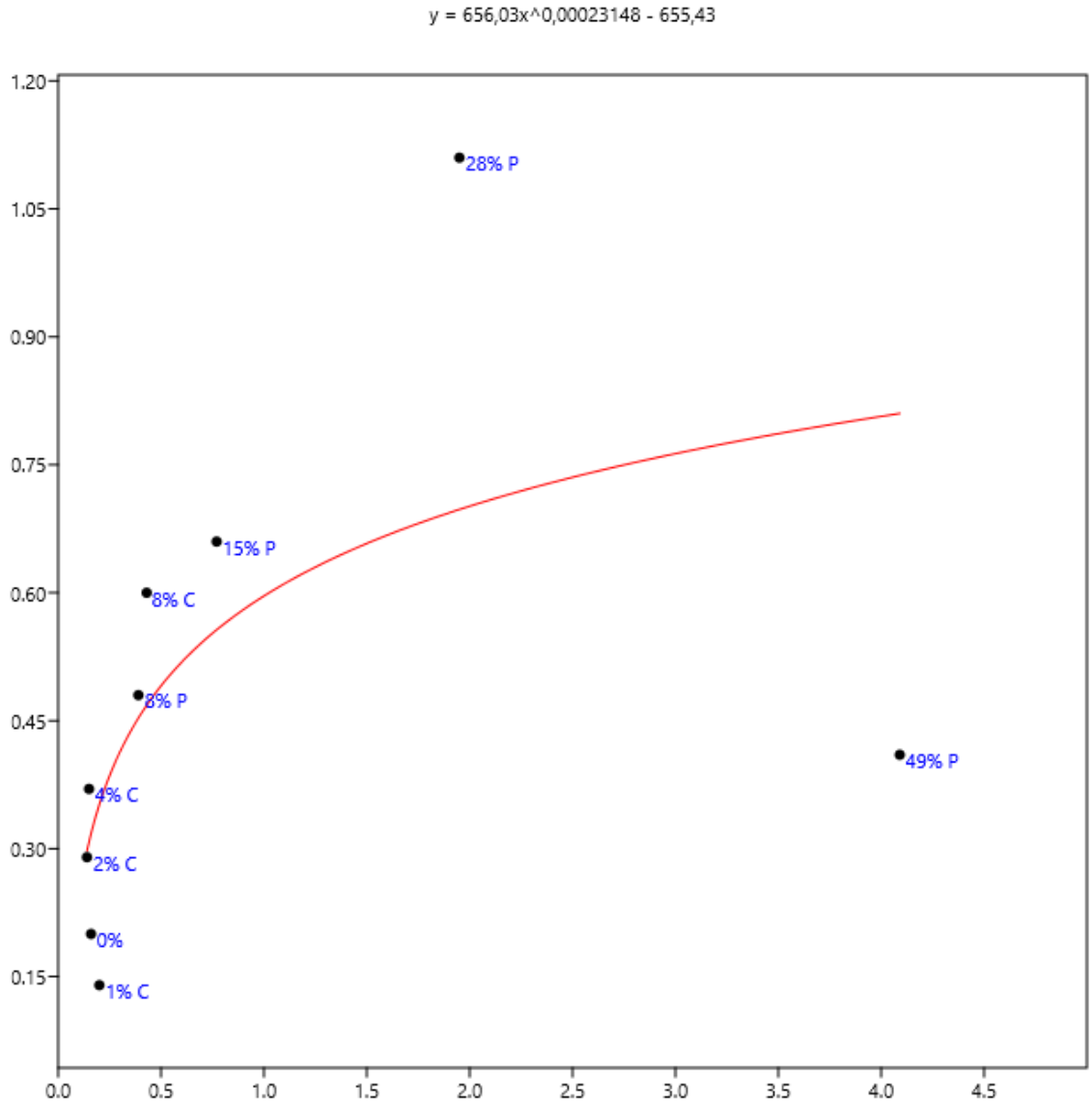

Figure 4.14. Correlation between biogenic silica and dissolved silica on the 7th day of the experiment in 2018.

4.4.2. 2019 experiment

In 2019 experiment it has been planned to get data about silica uptake from the PDMPO method and from the calculation as explained in “material and method” part. From the PDMPO method the obtained data from the quantitative analysis were close to zero and these results could not be used. More information about it can be found in the next chapter

“Discussion”. Nevertheless, the qualitative analysis worked quite well, but unfortunately being only qualitative, I got only some photos and, as an example, only one is shown in figure 4.15. There, the light-blue zones are areas where diatoms were depositing biogenic silica.

As for the quantitative analysis, not from PDMPO method, it has been possible to put the results in the graph in figure 16, where it is easy to understand that diatoms take up silica proportionally to the silicate/nitrate ratio. It shows an increasing trend during the first 5 days until the first peak, then the value tends to be quite constant. It is thus possible to understand that diatoms take up silicate with the same rate for the entire duration of the experiment after the first peak even if the biogenic silica and the diatom abundance increase or decrease.

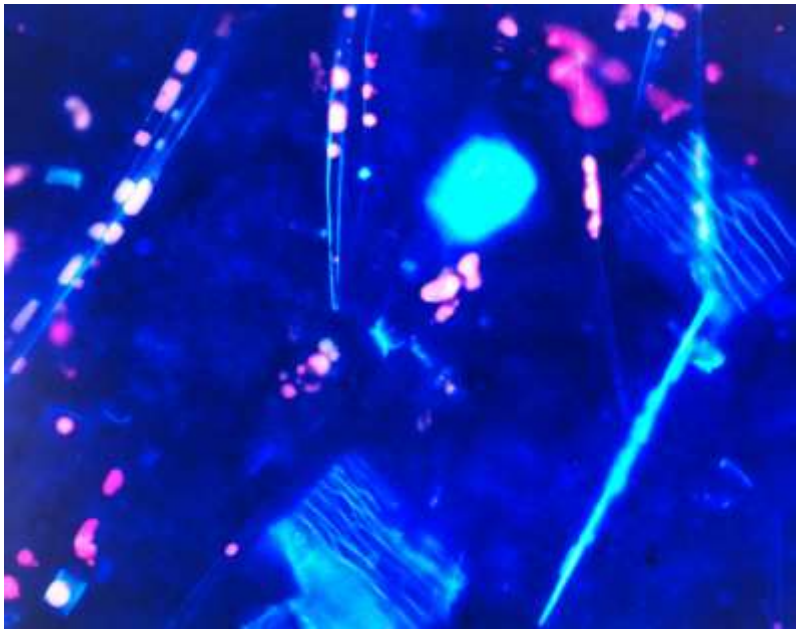

Figure 4.15. Photo at the ultraviolet microscopy (magnification= 63x).

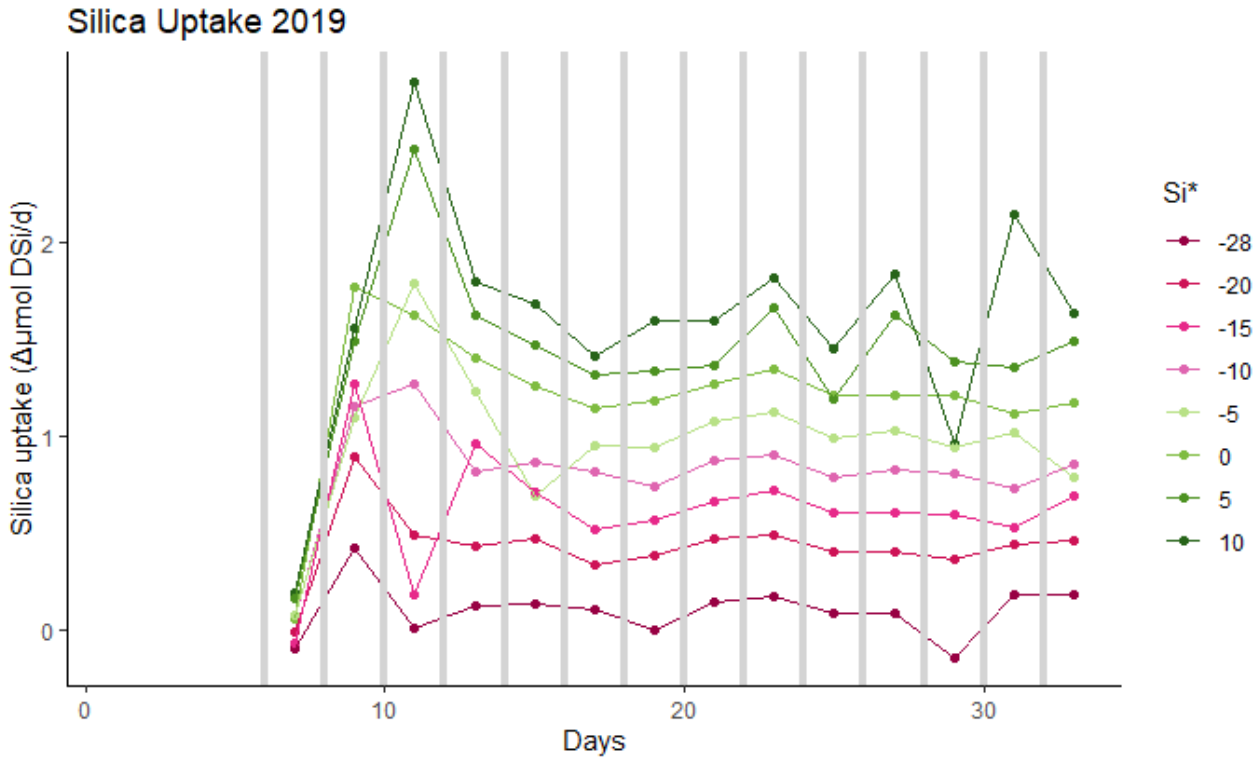

Figure 4.16. Temporal development of silica uptake during the 2018 experiment. Pink colours correspond to low Si* treatments and green for high Si* treatments. The grey bars in the background signal the deep-water addition events on days 6, 8, 10, 12, 14, 16, 18, 20, 22, 24, 26, 28, 30 and. The legend shows the value of Si* of the deep water added every two days.

Moreover, to explain better the silica uptake in relation to the gradient of Si*, below it is shown the correlation between dSi and bSi before the first deep water addition, on the 5th day (Fig. 4.17), and after 3 deep water addition on the 11th day (Fig. 4.18) that corresponds to the peak in silica uptake in the previous figure (Fig. 4.16). In the first correlation performed, it is possible to observe any distinction between the treatments, in fact no deep-water was added until day 6th. Here (Fig. 4.17) the equation is $\mathrm{bSi} = 0{,}36234\mathrm{dSi} + 0{,}33024\mu\frac{\mathrm{mol}}{\mathrm{L}}$, r^2=0,2095 and p=0,254, thus not significant. In the second picture (Fig. 18) it is possible to note the stable values in biogenic silica while dissolved silica values increase. Here (Fig. 4.18) the equation is $\mathrm{bSi} = -0{,}15863\mathrm{dSi} + 2{,}4399\mu\frac{\mathrm{mol}}{\mathrm{L}}$, the r^2= 0,00025522 and the p value is 0,96, thus not significant.

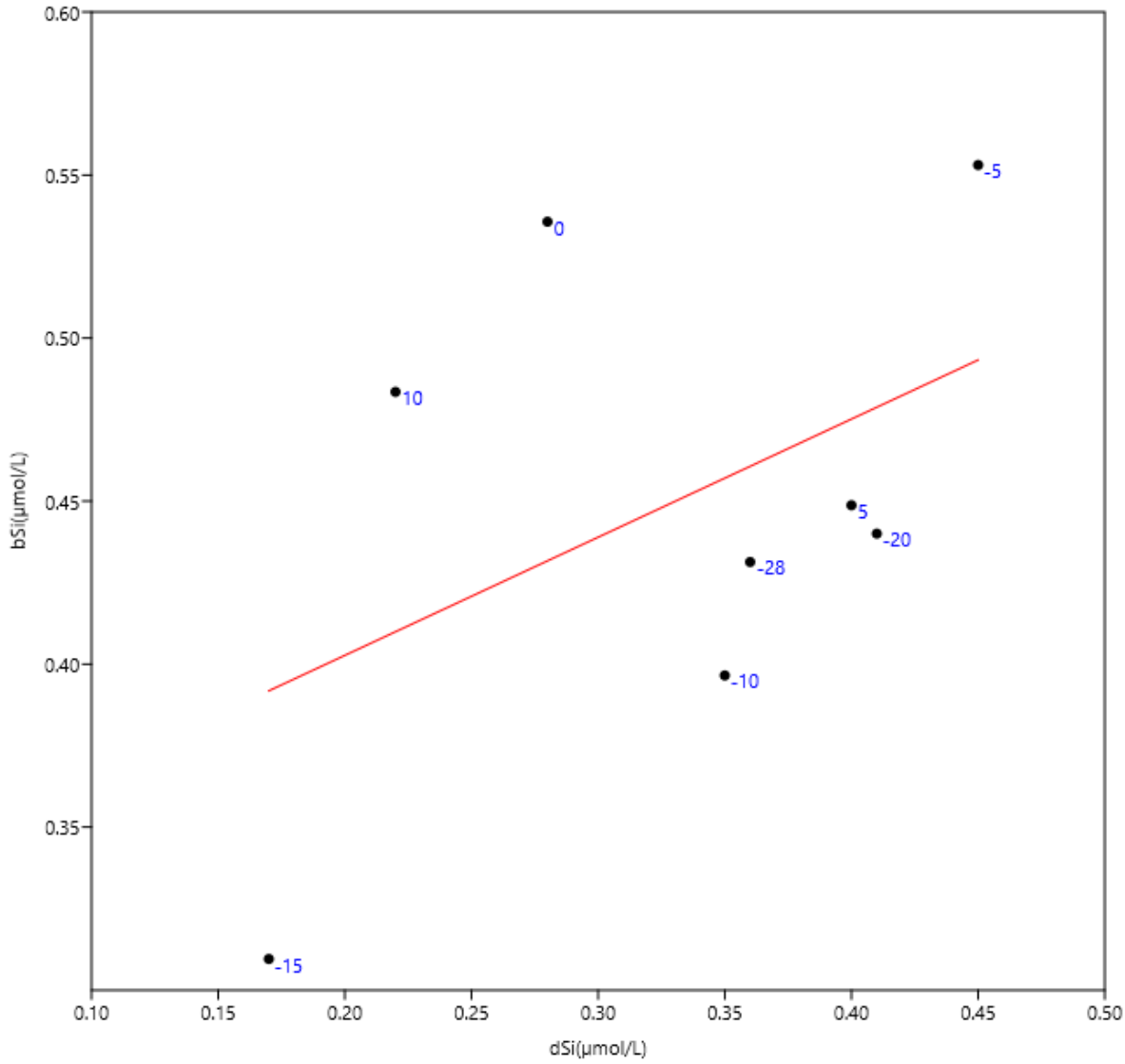

Figure 4.17. Correlation between biogenic silica and dissolved silica before the first deep water addition, on the 5th day in 2019 experiment.

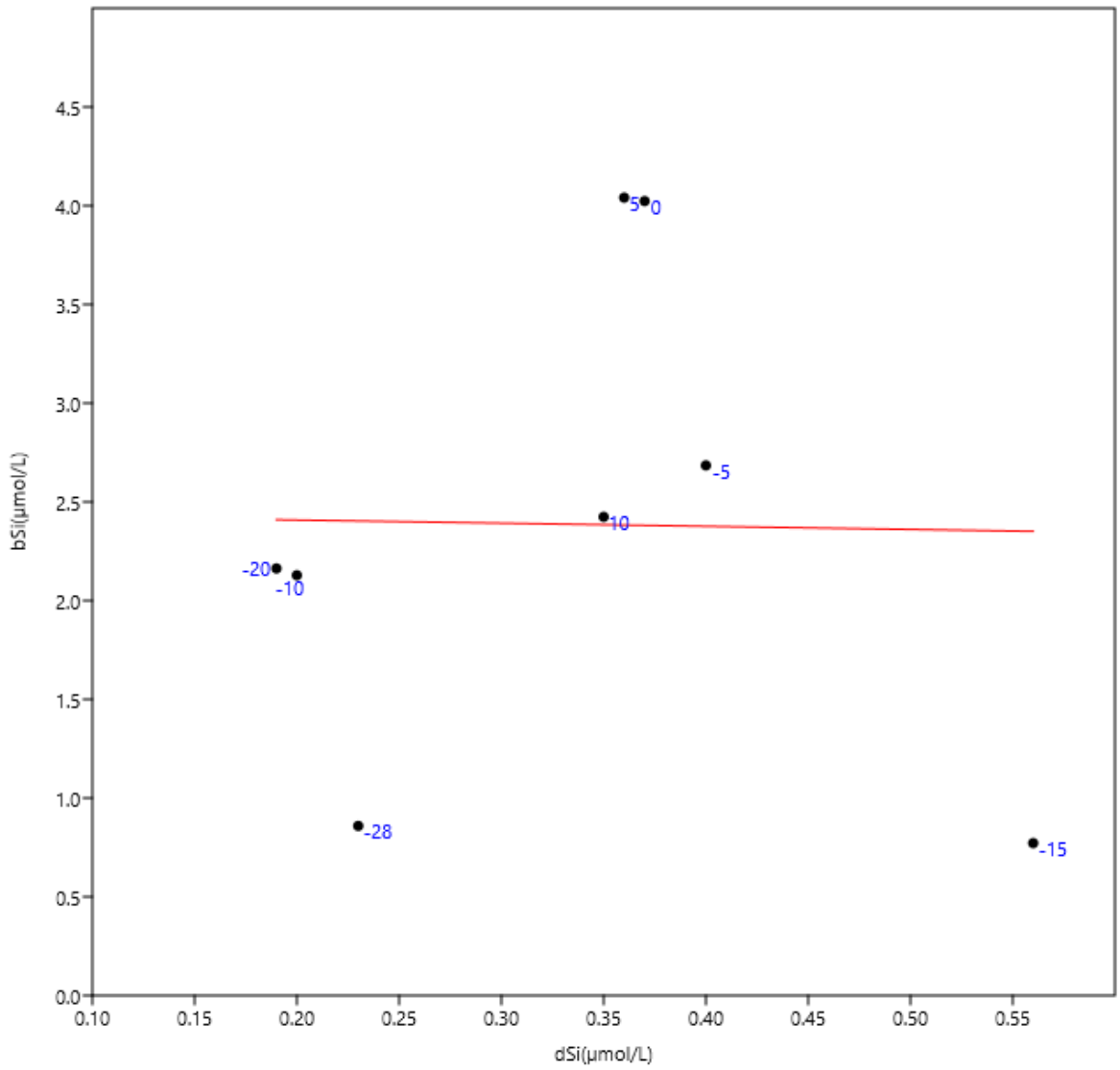

Figure 4.18. Correlation between biogenic silica and dissolved silica before the first first peak in silica uptake, after the 3rd deep water addition, on the 11th day in 2019 experiment.

4.5. Indicator of thickness

The $biogenic\ silica/\ diatom\ abundance$ ratio is an indicator of the quantity of biogenic silica contained in each diatom cell.

In 2018 (Fig. 4.21) this value is pretty constant except for some small peak and an increase in the end, meaning that diatom cells contain the same amount of biogenic silica during the entire duration of the experiment and also no differences can be found between the treatments.

In 2019 experiment (Fig. 4.23), diatoms show an increasing in biogenic silica per cell with increasing in Si* value. The figure shows a peak in the beginning followed by a constant value for each mesocosms. Thus, diatoms increase biogenic silica content with increasing in Si*, except for mesocosm with Si*=10. Moreover, looking at the zoomed chart from the 13th day until the end, even if the lines are not well separated, it is possible to note the major presence of high-silica treatments above the low-silicate treatments. (Fig. 4.23)

The two correlations performed show the relation between biogenic silica and diatom abundance, both integrated for the entire period of each experiment.

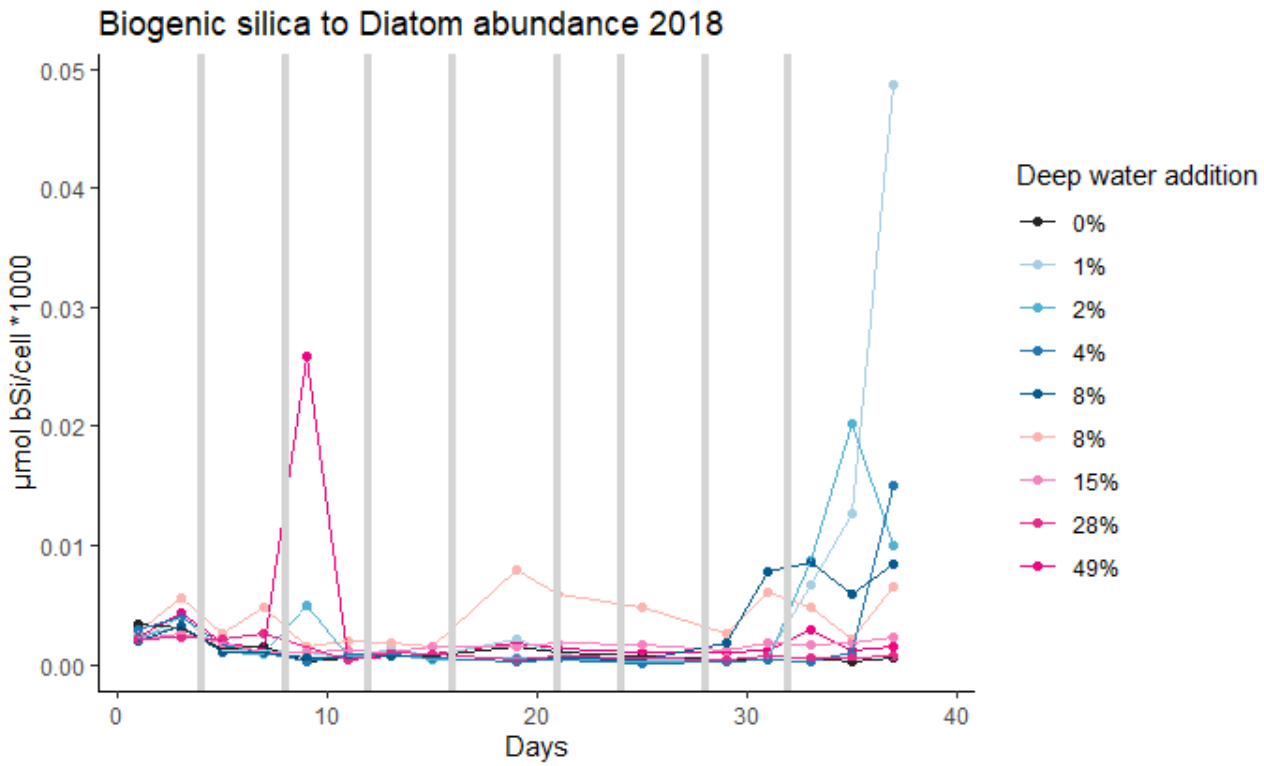

Figure 4.21. Temporal development of the bSiO2/diatom abundance ratio during the 2018 experiment. Black stands for the control in which no deep water was added, blue colours correspond to continuous treatments and pink for pulsed treatments. The grey bars in the background signal the deep-water addition events on date 4 the pulsed treatments and days 4, 8, 12, 16, 20, 24, 28 and 32 for the continuous treatments. The legend shows the percentage of water in each mesocosm that was substituted by nutrient-rich deep water per addition.

Looking at the two correlation, in 2018 experiment (Fig. 4.22) it is clear that keeping the Si:N ratio constant at 1:2, and varying the water exchange volume and mode, the ratio between biogenic silica and number of diatoms is constant. Specifically, the equation is $bSi = 0{,}00000058051(diatom\ abundance) + 2{,}669$, r^2=0,70217 and p value= 0,0058, thus this is highly significant. From the correlation plot of 2019 experiment (Fig. 4.24), an increasing in $biogenic\ silica/diatom\ abundance$ ratio occurs along the treatments from low silica to high silica treatments, even if the correlation is significant. Only the mesocosm with Si*=10 shows a different trend. Here (Fig. 4.24), the equation is $bSi = 0{,}00000011993\ diatom\ abundnace\left(\frac{Cell}{L}\right) + 22{,}149(\mu mol/L)$, with r^2= 0,48136 and p value of 0,028, meaning that it is significant.

Below (Fig. 4.22) it is represented the correlation, in 2018 experiment, between biogenic silica and diatom abundance integrated for the entire experimental period:

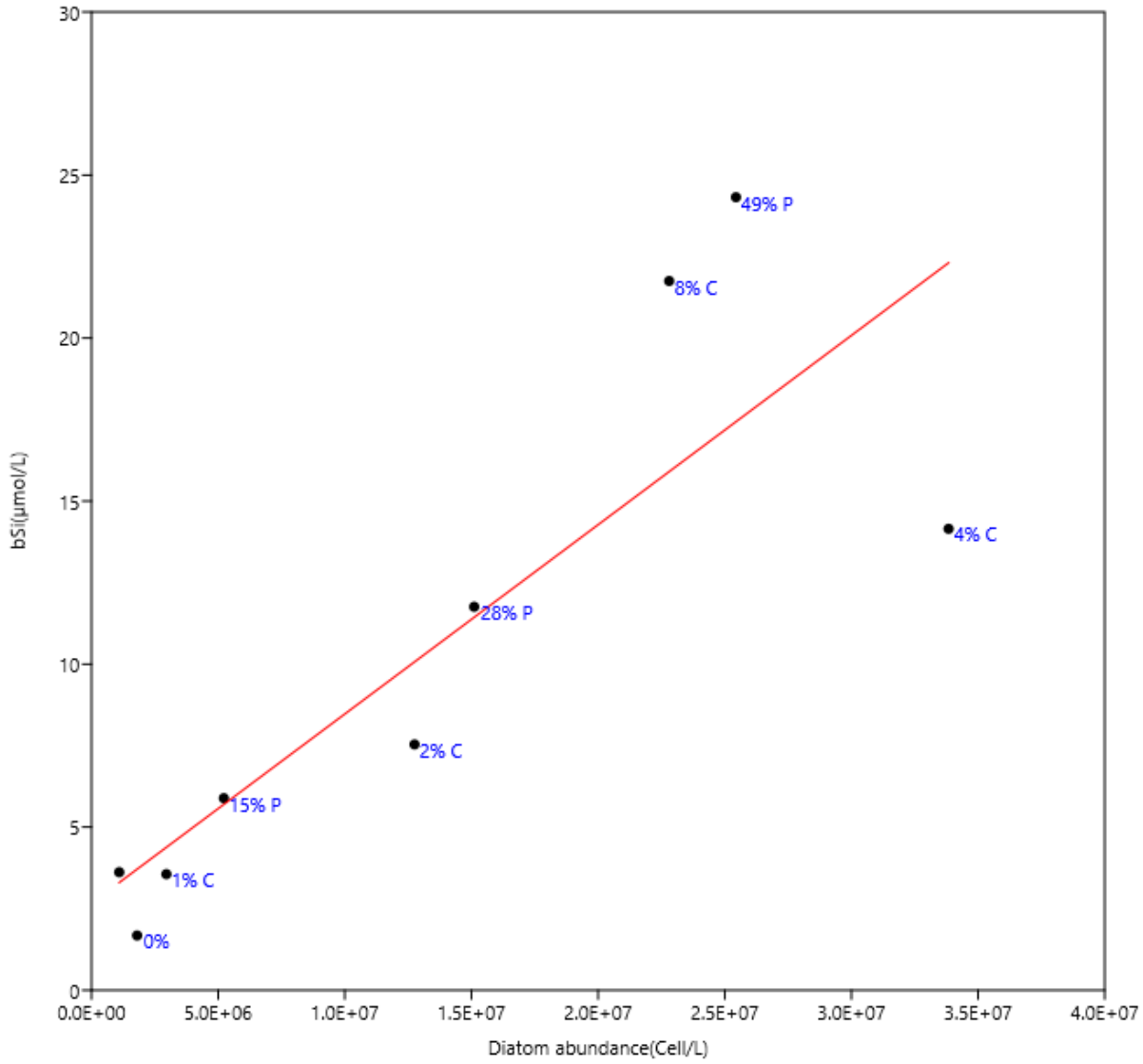

Figure 4.22. Correlation between biogenic silica and diatom abundance, integrated throughout experimental life. This graph is related to 2018 experiment.

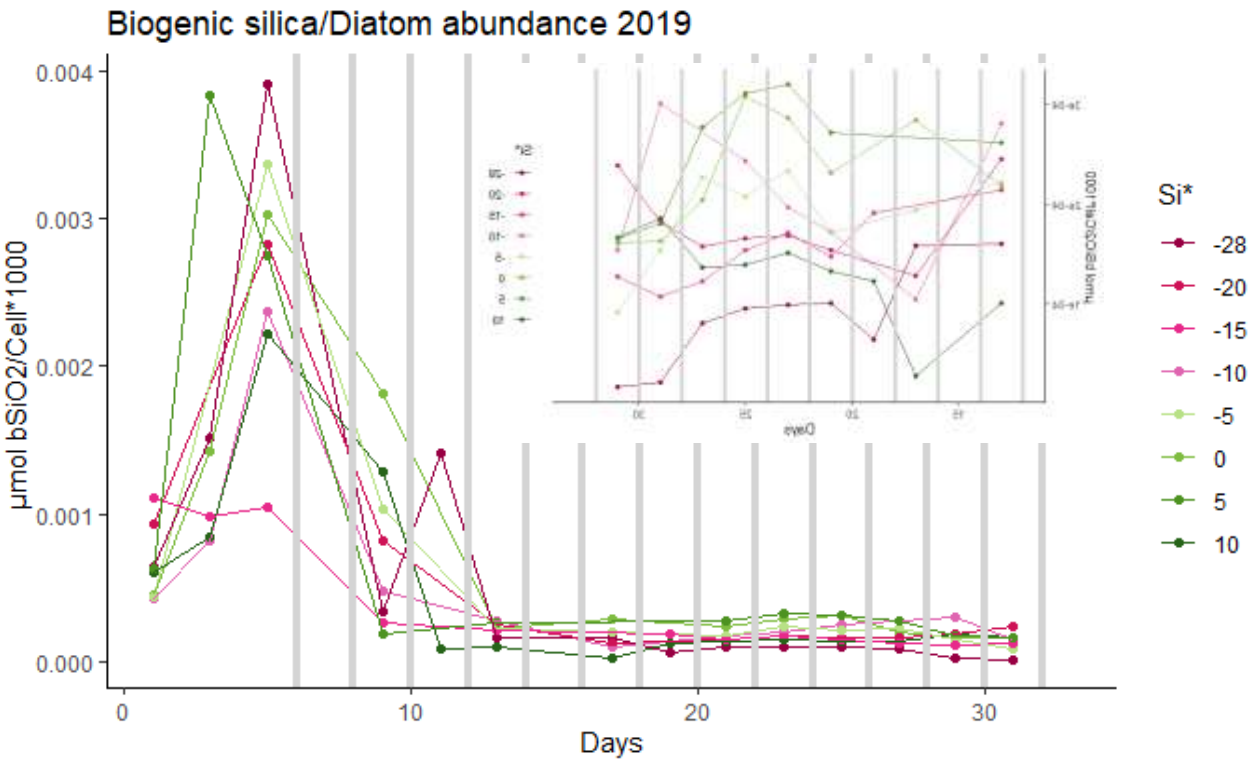

Figure 4.23. Temporal development of bSiO2/diatom abundance ratio during the 2019 experiment. Pink colours correspond to low Si* treatments and green for high Si* treatments. The grey bars in the background signal the deep-water addition events on days 6, 8, 10, 12, 14, 16, 18, 20, 22, 24, 26, 28, 30 and. The legend shows the value of Si* of the deep water added every two days. The small chart represents the same relation but from the 13th day until the end of the experiment, to zoom in.

Below (Fig. 4.24) it is represented the correlation, in 2019 experiment, between biogenic silica and diatom abundance integrated for the entire experimental period:

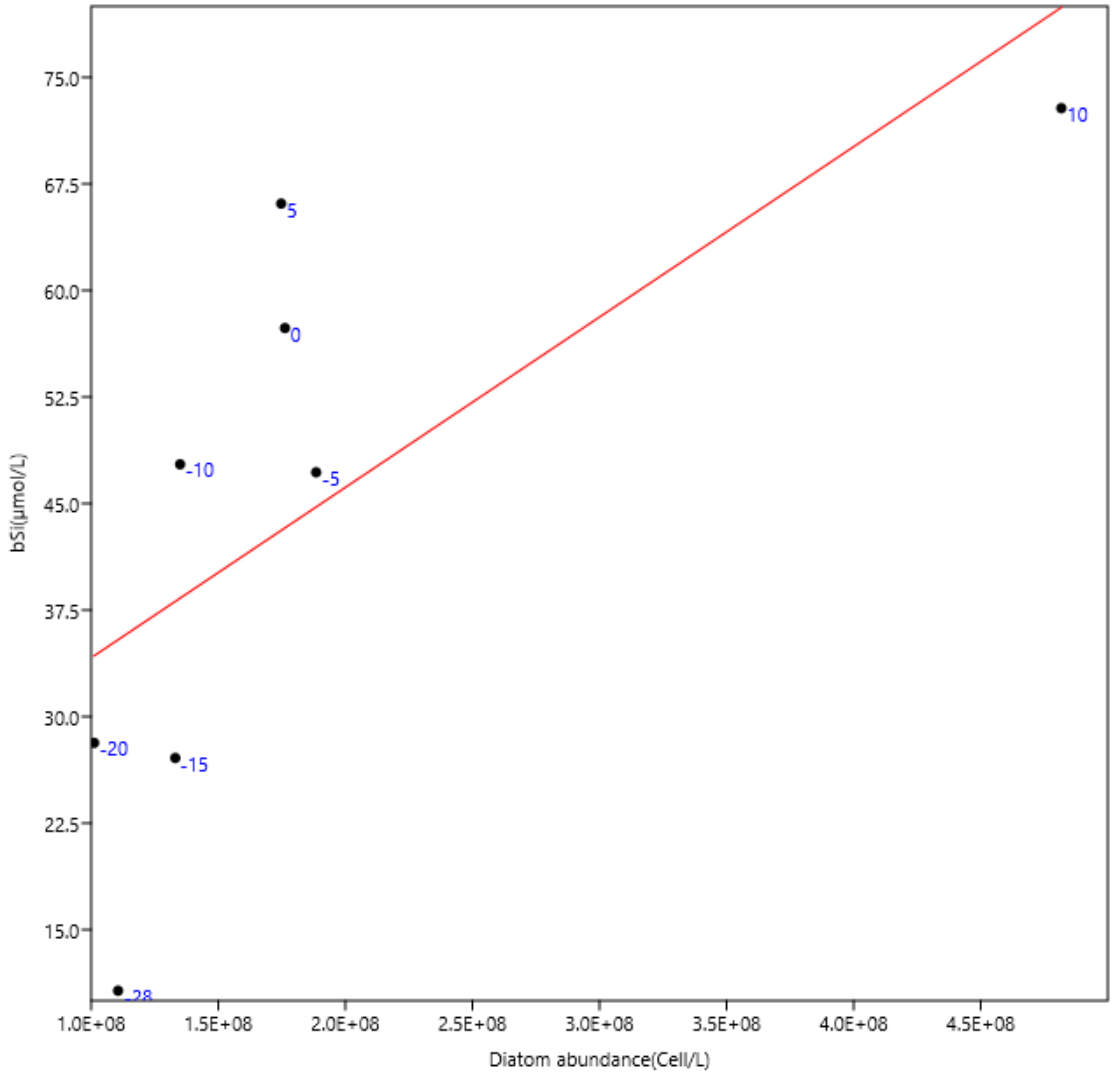

Figure 4.24. Correlation between biogenic silica and diatom abundance, integrated throughout experimental time. This graph is related to 2019 experiment.

4.6. Principal component analysis (PCA)

PCA was carried out to highlight, as an overview, the entire development over time of all the variables included in both experiments and thus to understand the effects of the uptake of dissolved silica by diatoms, as a consequence of different types of artificial upwelling systems.

The variables included are chlorophyll-a, biogenic silica (bSi), dissolved silica (dSi), diatom abundance, $biogenic\ silica/diatom\ abundance$ and chlorophyll-a(in µmol/L)/biogenic silica.

In 2018, it has been decided to divide the experiment in pulsed and continuous treatments, thus we got two PCA plots, one for pulsed treatments with control (Fig. 4.25) and one with continuous treatments with control (Fig. 4.26)

The first one is showed below:

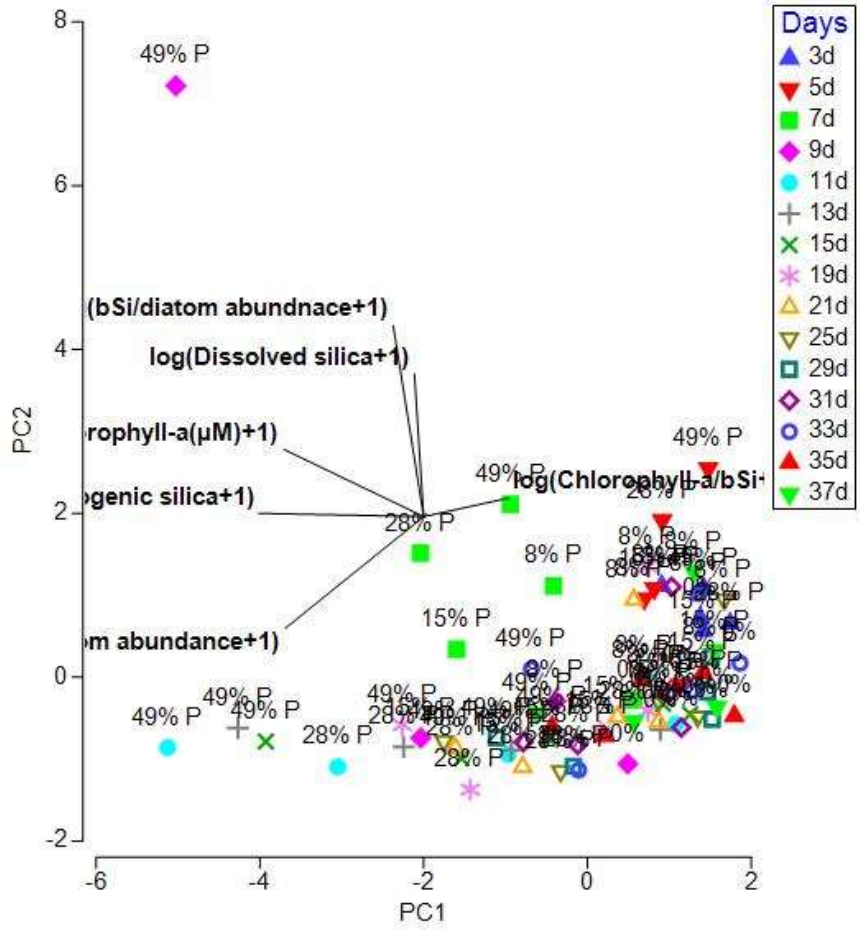

Figure 4.25. Principal component analysis for the pulsed treatments and control in 2018 experiment.

This principal component analysis (Fig. 4.25) has been carried out doing at first a transformation of all the variables with the function $\log(V+1)$, where V is a variable and then they have been normalized by $\frac{x-mean}{stdev}$, where x is the variable already transformed. In this PCA, the principal component1 (PC1) explains 43,6% of the entire variance, the principal component2 (PC2) explains the 24,7% of the entire variance, thus with the PC3, which explains the 16%, the first three principal components explain 84,3% of the entire variance. The PC1 is made up by $\log(bSi+1)$ with eigenvector of -0,606, $log(diatom\ abundance+1)$ with eigenvector of -0,508 and $log(Chlorophyll-a(\mu M)+1)$ with eigenvector of -0,513. The PC2 is made up by $\log(Dissolved\ silica+1)$ with eigenvector of 0,525 and by$\log\left(\frac{bSi}{diatom}abundance+1\right)$ with eigenvector of 0,701.

In this graph, three groups can be noted. One, who contains the mesocosms on the 7th day, one includes mesocosms on the 11th day and the biggest one that includes the mesocosms on the other days. These groups are congruent with the data shown before because the first group is aligned with the day of the peak in dissolved silica. The second one with the peak in bSi and the third one to the other days where all the variables tend to return to the values finding before the deep-water addition.

The second PCA analysis (Fig. 4.26) is shown below:

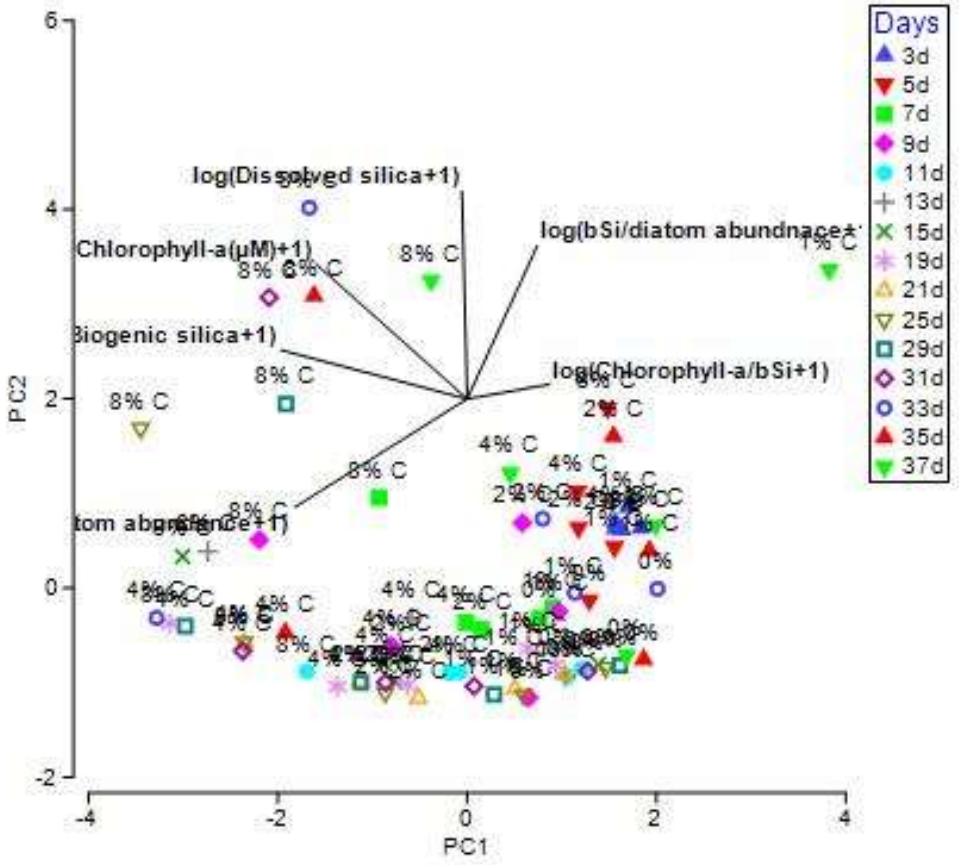

Figure 4.26. Principal component analysis for the continuous treatments and control in 2018 experiment.

This second principal component analysis (Fig. 4.26) has been carried out doing, as in the first one, the transformation of all the variables with the function $\log(V+1)$, followed by the normalization by $\frac{(x-mean)}{stdev}$.

In this PCA (Fig. 4.26), the PC1 explains 42,5%, while the PC2 explains 24,5% and the PC3 explains the 18,6% of the entire variance. These three, all together, represents the 85,6% of the entire variance. The PC 1 is made up $\log(Biogenic\ silica+1)$ with eigenvector of -0,592, $\log(Diatom\ abundance+1)$ with eigenvector of -0,548 and by $\log(\text{Chlorophyll}-\text{a}(\mu\text{M})+1)$ with eigenvector of -0,481. The PC2 is made up $\log(\text{Dissolved silica}+1)$ with eigenvector of 0,659, $log(bSi/diatom\ abundnace+1)$ with eigenvector of 0,486 and by $log(Chlorophyll\ a(\mu M)+1)$ with eigenvector of 0,429.

In this graph the outliers are represented for the most by the mesocosm with 8% of deep-water exchanged. The other points can be found inside a big group.

Below it is shown an overview with pulsed treatments, continuous treatments and control (Fig. 4.27). The transformation and normalization are the same of the previous principal component analyses. There, the PC 1 explains the 42,9% of the variance, the second one explains the 22,8% and the third one the 16,9%. The sum of the first three principal components explain in total the 82,6% of the entire variance. The first principal component, for the most, is made of $log(Biogenic\ silica + 1)$ with eigenvector of 0,592, $log(Diatom\ abundance + 1)$ with eigenvector of 0,551 and by $log(Chlorophyll - a(\mu M) + 1)$ with eigenvector 0,472. The second principal component is made up $log(Dissolved\ silica + 1)$ with eigenvector of 0,54 and by $log(bSi/diatom\ abundnace + 1)$ with eigenvector of 0,65.

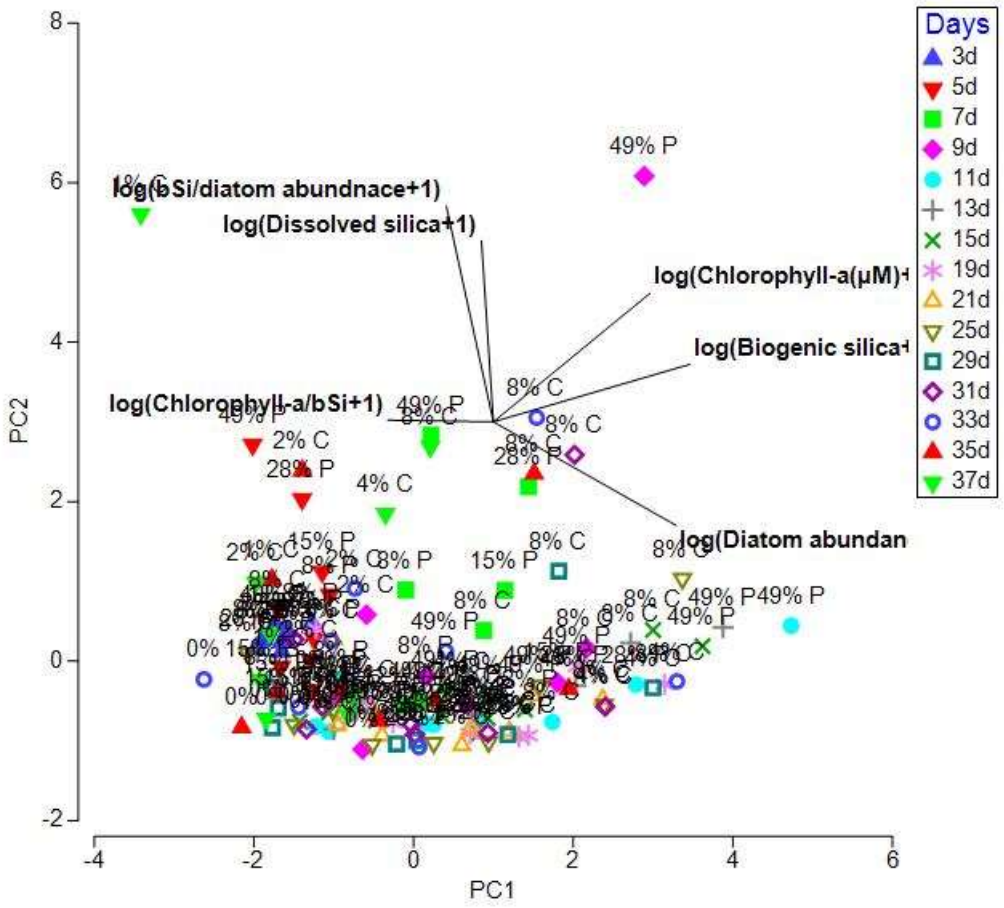

Figure 4.27 Principal component analysis for the pulsed treatments, continuous treatments and control in 2018 experiment.

For 2019 experiment, the PCA has been carried out before (Fig. 4.28) the first deep water addition and after it (Fig. 4.28), thus on the 5th day (Fig. 4.28), on the 9th day (Fig. 4.29) and also one for the entire period of the experiment (Fig. 4.30). In this experiment it has been decided to include in the principal component analysis the variables: dissolved silica, chlorophyllα, diatom abundance, $chlorophyll\alpha/biogenic\ silica$ $and\ biogenic\ silica/diatom\ abundance$. Biogenic silica is excluded due to high correlation with diatom abundance. In all the PCA analyses of the 2019 experiment the variable diatom abundance was transformed by the function $log(V+1)$, and then all the variables were normalized by $(x-mean)/stdev$. In the first PCA (Fig. 4.28), showed below, the first principal component explains the 95,7% of the entire variance, while the second principal component explains the 3,9%, both together represent the 99,6% of the entire variance. The first PC includes for the most $log(Biogenic\ Silica/Diatoms+1)$ with eigenvector of 0,961, diatom in this case means the abundance of diatoms. The second PC includes dissolved silica with eigenvector of -0,965. In this representation no group can be found.

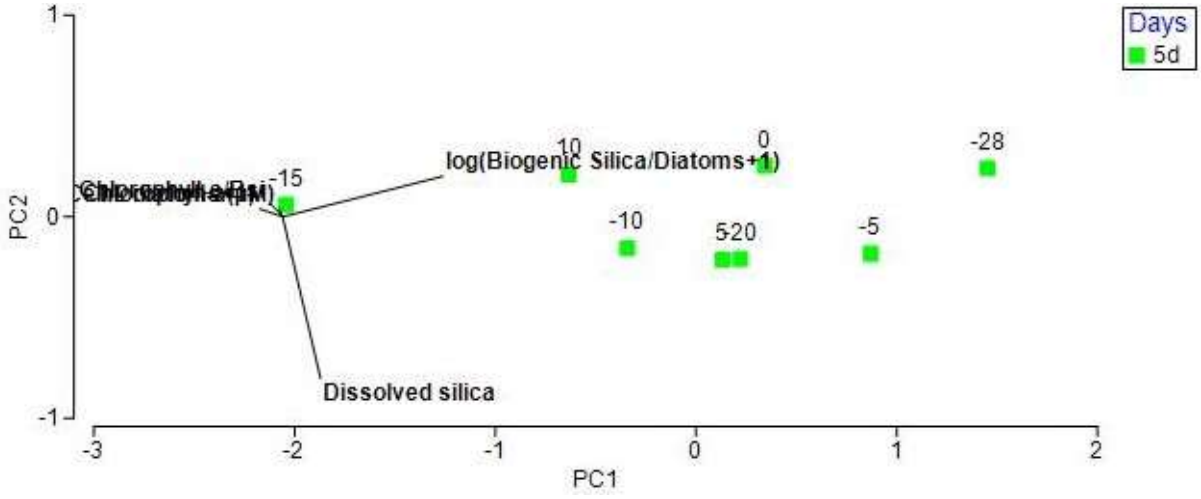

Figure 4.28. Principal component analysis for 5th day in 2019 experiment.

The second principal component analysis (Fig. 4.29) is shown below. In this, the first principal component explains the 86,8% of the entire variance, the second principal component explains the 11,8% of it, thus both together represent the 98,6% of the variance. Moreover, the first PC is represented by dissolved silica with eigenvector of

-0,991, the second PC by the $log(Biogenic\ Silica/Diatoms+1)$ with eigenvector of 0,875 and by $log(Cell/L\ diatoms+1)$ with eigenvector of -0,441. In this chart, the points

show a gradient along the first principal component. The high-silicate treatments are found on the left, while the low-silica treatments on the right.

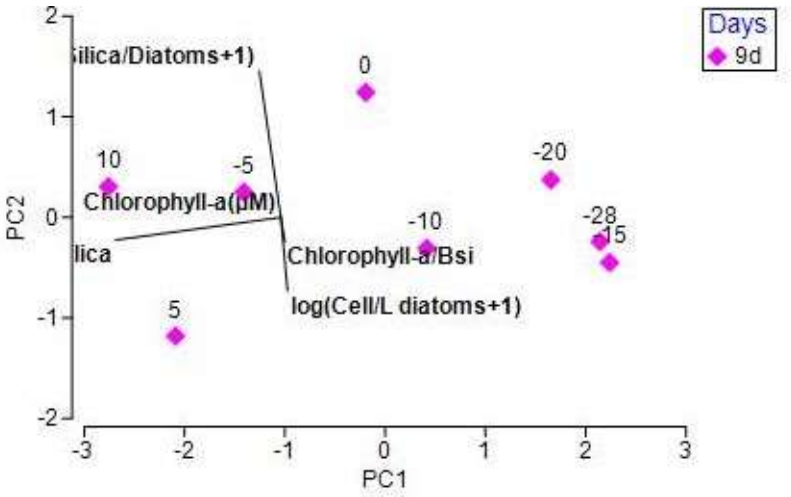

Figure 29. Principal component analysis for 9th day in 2019 experiment.

It has been made a principal component analysis for the entire period of the experiment, in order to summarize the development of these variables, that are useful and utilized to understand the silica uptake and the effects of it over time. In this PCA plot (Fig. 4.30), the first principal component explains the 60% of the entire variance, and the second one explains the 19,9%, both together explain the 79,9% of it. The first principal component is made up of $log(Cell/L\ diatoms + 1)$ with an eigenvector of 0,548, of $Chlorophyll - a(\mu M)$ with an eigenvector of 0,538 and of $log(Biogenic\ Silica/Diatoms + 1)$ with an eigenvector of -0,494. The second principal component is made up of $Chlorophyll - a/bSi$ with an eigenvector of 0,965. Here three groups can be found. The first one includes most of the mesocosms on the 1st, 3rd and 5th day, the second one the mesocosms on the 9th day and the third one includes the rest of the days. The 9th day represents a day of transition.

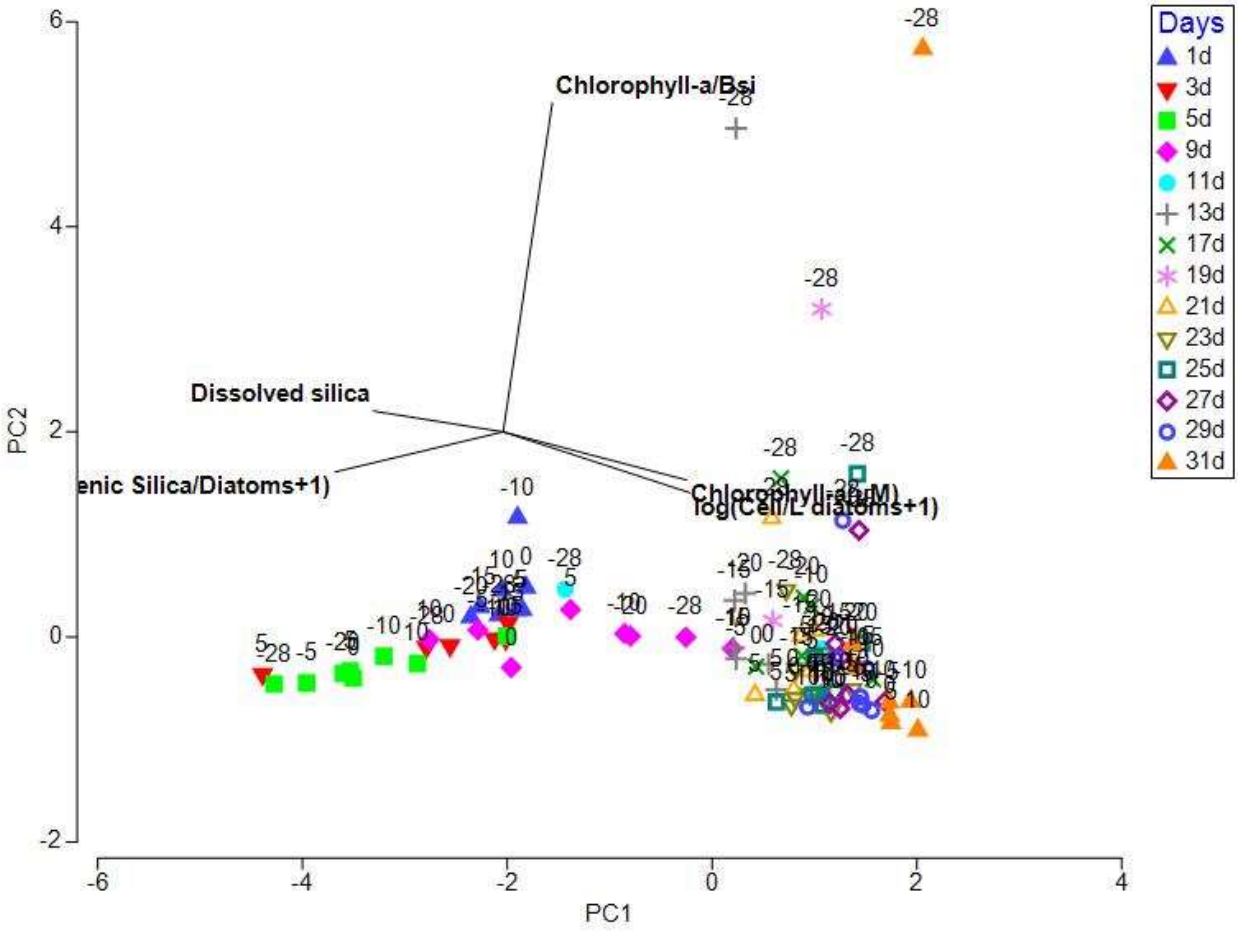

Figure 4.30. Principal component analysis for the entire experimental period of 2019 experiment.

5. Discussion

Two different experiments were conducted to highlight the silica uptake in mesocosm studies performed in the Canary Islands. Both experiments show similarity in the general concept: artificial upwelling performed as a mitigation action against climate change, in order to increase fish production in a sustainable way and possibly sequester atmospheric CO2 into the deep ocean layer. The first experiment, made in 2018, was performed with nine mesocosms divided by the upwelling mode in three groups: one composed of four mesocosms which experienced one single addition of deep-water (pulsed mode), one composed of four mesocosms which experienced the deep-water addition every four day (continuous mode) and one mesocosm kept untreated as control. In both groups a gradient in intensity of upwelling was performed. The target intensities of deep water were 0% for control, 1%, 2%, 4%, 8% for mesocosms in continuous mode and 8%, 15%, 28% and 49% for pulsed mode.

Moreover, this mesocosm experiment was made in the way that in couple (pulsed and continuous) they received the same amount of deep-water along the entire duration of the experiment.

The second experiment, conducted in 2019, was composed of eight mesocosms, where all of them experienced the deep-water addition every 2 days with an exchange of 4% in volume. Here, a gradient in Si* in deep water addition was performed along the mesocosms. The Riebesell team with the term “Si*” means the difference between Silica and Nitrate concentration (Si*=[Silicate]-[Nitrate]). The Si* values applied were -28, -20, -15, -10, -5, 0, 5, 10. This study is aimed to answer mainly the three questions reported before, to make advices on future study and to propose future experiments in order to increase fish production and enhance the carbon sequestration through the artificial upwelling system.

5.1. Silica uptake under pulsed and continuous upwelling

In order to answer the first question, about the differences in silica uptake between pulsed and continuous upwelling systems, it is necessary to look at the results of the experiment conducted in 2018 about dissolved silica (Fig. 4.1), biogenic silica (Fig. 4.3), diatom abundance (Fig . 4.5) and, most importantly, the silica uptake development over time.

In the figure about dissolved silica (Fig.4.1), the first peak appears right after the first deep water addition. The height of the dissolved silica concentration reached follows the amount of deep water added. Then, the following deep-water additions do not increase the dissolved silica value as occurred with the first one. This mean that the phytoplankton community uptakes silica more effectively after the first addition, in other words: phytoplankton community change itself along the experiments in order to maximize the uptake of silica. This trend has been found also in the other results, in the one about silica-uptake (Fig.4.9), where the mesocosms with the pulsed mode treatment show the uptake only right after the deep-water addition, while the continuous treatments show a stable development of silica uptake values. In results of biogenic silica temporal development (Fig.4.3), values reach a maximum 3 days after the deep-water addition in the pulsed mode, instead in the continuous mode this value shows and increasing or stable trend along the experiment, except in the end when a coccolithophore bloom occurs (from not published data of GEOMAR Helmholtz Centre for Ocean Research, Kiel). Moreover, in order to differently quantify the silica uptake, the integration of biogenic silica in each treatment over time has been also calculated. Diatom abundance shows similar trend to biogenic silica even if a higher noise is observed. This is interesting since the 2018 experiment was built in order to bring about the same amount of nutrients including silica in pulsed and continuous treatments, in couple. From this, the integrated values are shown below as a summary:

Control	bSi(µmol/L)	Continuous	bSi(µmol/L)	Pulsed	bSi(µmol/L)
	1,6809	1%	3,558306	8%	3,619109
		2%	7,536084	15%	5,885327
		4%	14,14838	28%	11,75891
		8%	21,74843	49%	24,32466
Sum			46,99119		45,58801

From this result, the differences between pulsed and continuous mode, is not wide for biogenic silica, even if continuous mode prevails, this means that, since dissolved silica is taken up and converted into biogenic silica, in continuous mode the biogenic silica production is higher than in the pulsed treatments, and thus the silica uptake is higher in continuous mode than in the pulsed one, or better, the conversion of dissolved silica into biogenic silica is higher in continuous mode. Moreover, the big changes occurring in phytoplankton community between continuous and in pulsed treatments can be noted in the diatom abundance figure (Fig. 4.5), where in the pulsed treatments one peak occurs,

followed by a decline, while in continuous treatments the diatom community tends to remain for a longer time, sustained by frequent deep-water addition. The changes between the two modes are also shown, as an overview, by PCA (Fig. 4.25) where in pulsed treatments all the variables, after the deep-water addition, tend to return to the values before the addition. The PCA regarding the continuous mode highlights a "migration" of the phytoplankton community toward higher values in PC1, and again, since the PC1 is made up for the most by $\log(Biogenic\ silica + 1)$ and $\log(Diatom\ abundance + 1)$, diatoms increase their community and biogenic silica production in continuous upwelling. In conclusion, it means that the phytoplankton community, grown in continuous upwelling system, takes up silica about at the same rate along the experiments, and that diatoms show a constant presence. In a wider view, continuous mode could sustain a sustainable fish production since artificial upwelling mimics the natural upwelling and produce the base of the marine food chain, the diatoms. More studies are needed to understand if and how continuous upwelling system can sustain a trophic chain which leads to an increase in fish production.

5.2. Influence of Si* on silica uptake

In order to answer to the second question: "Does increasing Si* enhance the silica uptake?" we must take into account, first of all, the results shown in figure 4.16. In this graph, silica uptake values show an increasing trend along the treatments, in the following range of Si* provided: -28≤Si*≤10. It can be noted that the values of silica uptake reach the first and the only peak 3-5 days after the deep-water addition, then remain stable. Moreover, the low-silica treatments show the maximum earlier than the high-silica treatments. This may mean that the amount of silicate given in the high-silica treatment could be too much to reach the peak of the uptake in 3 days, while the diatom community in low-silica treatments reach it in 3 days. Thus, the diatom community responds to silica availability with different N:Si ratio (Si*) in deep-water in upwelling system. Presumably, this is carried out in four ways: i) increasing in cell number and ii) cell size, iii) increasing in store of dissolved silica and iv) in production of biogenic silica as frustules. This hypothesis could be explained looking at the figure of diatom abundance (Fig.4. 6), keeping in mind also the results on silica uptake (Fig. 4.16), the curves of the same mesocosms do not really show different trends, except for the one with Si* value of 10. This could be explained in part according to McNair et al. (2018): in silica-limiting conditions, as occurred in low silica treatments, diatoms reduce silicification to maintain

the cell division rate. In addition, a density effect could also occur. This is the reason why the diatom abundance curves show similar values along the mesocosms, except for the highest value of the high silica treatment group. In addition, this also find confirmation in the results of biogenic silica (Fig. 4.4), where the curves of low-silica treatments show stable trend or slightly decreasing, while the ones of diatom abundance show a continuous increasing trend. This lower silicification in low-silica treatments has an ecological impact on the grazing by copepods, as they will be favoured. Moreover, from the principal component analysis (PCA), made before the first deep-water addition for all the mesocosms, it appears chaotically arranged, while after two deep-water addition the mesocosms are on a gradient along the principal component1, from the highest Si* value to the lowest one, where the PC1 is composed for the most by dissolved silica. From the PCA for the entire period, all the mesocosms, except the one of Si*=-28, show a temporal gradient along PC1(made up diatom abundance, chlorophyllα and bSi/ diatom abundance). The PCA data confirm that phytoplankton community uptake Si and that a shift in phytoplankton community occurs.

5.3. Possibility of influence of amount of deep water added and the N:Si ratio on the biogenic silica/ diatom abundance ratio

The ratio between biogenic silica and diatom abundance has been built as an indicator of the silicification of the diatom cellular wall. It has been thought in this way since from McNair et al., (2018) it appears that the silica content influences the marine food web and hence the biogeochemical cycle of carbon and silicon. This indicator was calculated for both experiments. It is represented by a scatter plot where in y-axis biogenic silica values and in x-axis the diatom abundance values are shown, both values are integrated for the entire experimental duration. In the experiment conducted in the autumn of 2018, a high positive correlation between these two variables was found with p value= 0,0058 (Fig. 4.22). The temporal development of this ratio in 2018 experiment (Fig. 4. 21) shows some noise, maybe due to some uncertainty in diatom cell counts, as it can be noted in the figure 5. Difficulties in finding differences between treatments in 2018 temporal development may be experienced. These two figures (Fig. 4.21 & 4.22) highlight the fact that an upwelling with different mode (pulsed or continuous) but with the same Si:N ratio (1:2) leads to the same biogenic silica/diatom abundance ratio. Therefore, the type of

artificial upwelling (amount of water and frequency of addition) may not influence the diatom silica content. On the other hand, from figure 4.21, about diatom silica content over time, the pulsed treatments appear to show values above the ones of continuous treatments. It is very difficult to deduce more finding from this figure since noise occurs. Moreover, this finding could agree with that of Claquin et al. (2002), which explains that biogenic silica per cell tends to increase with decreasing growth rate. This is what happened in pulsed treatments over the peak in diatom abundance. Thus, more studies also on the fate of diatoms with different type of artificial upwelling are needed, in order to highlight the best artificial upwelling mode.

In the experiment conducted in Summer 2019, the temporal development of the diatom silica content (Fig. 4.23) shows a peak right before the first deep-water addition. It means that keeping the diatoms into a stable water leads to a rapid decline in nutrient concentration (Fig.4. 2) with the decline in diatom abundance as a consequence. In addition, their predators, the copepods, may have had a negative effect on diatom population in this part of the experiment. From the first deep water addition, the curves of the mesocosms are found quite in a gradient along the y-axis (where y=bSi/diatom abundance), except for the highest high-silica treatment which shows particular trend in diatom abundance. In the scatter plot of biogenic silica to diatom abundance, the correlation between these two variables is significative, even if taking out of consideration the value corresponding to Si*=10, the diatom silica content tends to increase with Si* value. This could be interpreted as follows: more silica is given, more diatom cells are produced and more silicification occurs. This find confirmation in McNair et al. (2018) where silica limited conditions lead to decrease silicification to maintain the growth. Moreover, the figure of diatom abundance (Fig. 5&6) do not show a clear difference between treatments. This could be explained by also a cell density effect that leads to a not excessive growth of diatoms. Thus, since the silica-uptake increase with the dissolved silica given, and the diatom population does not show differences between the treatments, the diatoms in high-silica treatments have to increase the silicification process, hence the frustules will be bigger and thicker. This finding is similar to the one observed by Martin-Jézéquel et al. (2000), thus more silica is available especially for a prolongated cell cycle phase, more silica will be incorporated into the diatom cell wall. This will have repercussions on pelagic food web as well on potential carbon sequestration.

5.4. Experimental limitation

These two experiments show some uncertainty. Both experiments are thought to represent, through mesocosms, the entire water column but in a small volume, especially in 2019, thus the pelagic food web could show different dynamics respect to what occurs in nature due to the small number of the individuals. Moreover, some effects could derive from the plastic composition of the mesocosm bag. Some errors could have been occurred in each analysis, since they were done also by students. All of these datas are preliminaries, thus the errors were not taken into account. In particular, in 2019 experiment the student, followed by the tutor, made the PDMPO method with some arrangements. They were needed since the instrumental equipment in Gran Canaria did not comprise the specific ones for this method. Specifically, even if the PDMPO dye is light-sensitive, not so many adroitness were taken, moreover the length of the filtration process were often very long, maybe something could have been happened there. The storage of the filter was longer than 24 hours. The Teflon rod was unusable since the supernatant methanol tended to go out, thus it was taken out with pipette. In addition, the dry process was longer than the one of the protocol due to the different kind of oven available. All of these aspects could have produced errors and anomalous data.

5.5. Artificial upwelling as mitigation action against fish production decline and to enhance the oceanic carbon sequestration.

Nowadays, ocean is getting more attention on its vulnerability due to global changing (Keith Brander 2010) and its role against climate change. In this contest, of declining in oceanic productivity and fish production within the end of this century, the European project “Ocean Art-Up” was thought. This project, in order to increase fish production and to highlight possible consequences on carbon sequestration, was built as mesocosm experiments having in common artificial upwelling. In the 2018 research campaign two mode, pulsed and continuous, were analysed, while in 2019 different Si:N ratio in artificial upwelling were experienced. From the last two experiments and the knowledge in the literature, a clear correlation between deep water addition and diatom growth clearly appears. This finding is in line with the most efficient marine pelagic food chain, which is

composed of diatoms at the first trophic level, copepods at the second one and then planktivorous fish and primary predatory fish at 3rd and 4th level respectively (Sommer et al., 2002). Moreover, also carbon sequestration is partially explained by this data since, if diatoms are not grazed, they will tend to sink to the deep ocean layer with downward transport of significant amounts of carbon and silicon in according to previous papers (Beaulieu and Smith 1998; Armbrust 2009).

In order contrast the decline in fish production, which is affecting almost the entire oceanic surface and human population that live from it, it is necessary to make the local pelagic trophic chain more efficient. This could be done through this system since it moves the deep water upward to the surface trying to nullify the stratification of the water (increasingly occurring due to climate change). In this way high concentration in nutrients occurs in the surface, in particular of silicon, with consequent increase in diatom abundance, in according to Aure et al., (2007). Specifically, from the data explained before a probably increase in fish production can be realized but with some adroitness. The water included in upwelling process must not show high Si:N ratio. This is in contrast to the finding of Sommer et al. (2002). This is due to the influences of diatoms on copepod population, since copepod population needs to be fed by the planktivorous fish. Copepods with their nauplii prefer diatoms with low silica content over high silica-containing cells, as explained by Liu et al., (2016) Moreover, high silica diatom content is related to a reduction of egg production rate and hatching, maybe due to toxic aldehydes production (Miralto et al., 1999). These two factors can be explained by increasing in diatom silica content, which is linked to the silicification level of frustules, which are defence traits against grazers (Friedrichs et al., 2013) and do not provide any nutritional value for zooplankton (Liu et al., 2016).

From this findings, prolonged artificial upwelling with high Si:N ratio leads to a potential carbon sequestration. This can be the consequence of the production of large diatoms with heavy silicification (Van Nieuwerburgh et al. (2004). These diatoms will be not grazed by copepods, thus this phytoplanktonic biomass may sink to the deeper layer in the ocean. Moreover, from Liu and Wu (2016), the copepod pellets from high silica containing diatoms show higher sinking rate than fecal pellets from copepods feeding on low silica containing diatoms. Similar findings are shown by Bienfang (1980). Therefore, the formers are more likely to sink out of the mixed layer before being degraded (Liu and Wu, 2016). In conclusion the most efficient food web may be appear right after the first deep-

water addition, at the beginning of the bloom. The transport of biomass along the pelagic food chain may be maintained in continuous upwelling with low Si:N ratio. Upwelling with high Si:N ratio, in particular later than the beginning of the bloom, leads to the sink of diatom biomass, thus if the carbon downward flux exceeds the carbon upward flux linked to the upwelling, it will result in carbon sequestration. More studies on the relation of sinking diatoms and carbon sequestration in artificial upwelling systems are needed since the ocean is getting the anthropogenic carbon released. In any case, artificial upwelling system leads to the reduction of oceanic surface temperature.

6. Bibliography

Abrantes, Fatima, Pedro Cermeno, Cristina Lopes, Oscar Romero, Lélia Matos, Jolanda Van Iperen, Marta Rufino, and Vitor Magalhães, 2016. Diatoms Si Uptake Capacity Drives Carbon Export in Coastal Upwelling Systems. Biogeosciences 13, no. 14: 4099–4109. https://doi.org/10.5194/bg-13-4099-2016.

Arístegui, J., P. Tett, A. Hernández-Guerra, G. Basterretxea, M.F. Montero, K. Wild, P. Sangrá, et al, 1997. The Influence of Island-Generated Eddies on Chlorophyll Distribution: A Study of Mesoscale Variation around Gran Canaria. Deep Sea Research Part I: Oceanographic Research Papers 44, no. 1: 71–96. https://doi.org/10.1016/S0967-0637(96)00093-3.

Arístegui, Javier, Eric D. Barton, Xosé A. Álvarez-Salgado, A. Miguel P. Santos, Francisco G. Figueiras, Souad Kifani, Santiago Hernández-León, Evan Mason, Eric Machú, and Hervé Demarcq, 2009. Sub-Regional Ecosystem Variability in the Canary Current Upwelling. Progress in Oceanography 83, no. 1–4: 33–48. https://doi.org/10.1016/j.pocean.2009.07.031.

Aure, J., Strand, ø, Erga, S., Strohmeier, T., 2007. Primary production enhancement by artificial upwelling in a western Norwegian fjord. Marine Ecology Progress Series 352, 39–52. https://doi.org/10.3354/meps07139

Ban, S., Burns, C., Castel, J., Chaudron, Y., Christou, E., Escribano, R., Fonda Umani, S., Gasparini, S., Guerrero-Ruiz, F., Hoffmeyer, M., Ianora, A., Kang, H.K., Laabir, M., Lacoste, A., Miralto, A., Ning, X., Poulet, S., Rodriguez, V., Runge, J., Shi, J., Starr, M., Uye, S., Wang, Y., 1997. The paradox of diatom — copepod interactions. Mar. Ecol. Prog. Ser. 157, 287–293.

Barbier, Edward B, 2017. Marine Ecosystem Services. Current Biology 27, no. 11: R507–10. https://doi.org/10.1016/j.cub.2017.03.020.

Barton, E.D., Arístegui, J., Tett, P., Cantón, M., García-Braun, J., Hernández-León, S., Nykjaer, L., Almeida, C., Almunia, J., Ballesteros, S., et al., 1998. The transition zone of the Canary Current upwelling region. Prog. Oceanogr. 41, 455–504

Basterretxea, G, and J Arístegui, 2000. Mesoscale Variability in Phytoplankton Biomass Distribution and Photosynthetic Parameters in the Canary-NW African Coastal Transition Zone. Marine Ecology Progress Series 197: 27–40. https://doi.org/10.3354/meps197027.

Bauman, S., Costa, M., Fong, M., House, B., Perez, E., Tan, M., Thornton, A., Franks, P., 2014. Augmenting the Biological Pump: The Shortcomings of Geoengineered Upwelling. Oceanography 27, 17–23. https://doi.org/10.5670/oceanog.2014.79

Beaulieu, S. E., and K. L. Smith. 1998. Phytodetritus entering the benthic boundary layer and aggregated on the sea floor in the abyssal NE Pacific: Macro- and microscopic composition. Deep-Sea Res. Part II 45: 781–815, doi:10.1016/ S0967-0645(98)00003-4

Bienfang, P. K, 1980. Herbivore Diet Affects Fecal Pellet Settling. Canadian Journal of

Fisheries and Aquatic Sciences 37, no. 9: 1352–57. https://doi.org/10.1139/f80-173.

Bienfang, P. K., Harrison, P. J. & Quarmby, L. M. 1982. Sinking rate response to depletion of nitrate, phosphate and silicate in four marine diatoms. Mar. Biol. 67:295–302.

Bopp, L., O. Aumont, P. Cadule, S. Alvain, and M. Gehlen, 2005. Response of Diatoms Distribution to Global Warming and Potential Implications: A Global Model Study: DIATOMS AND CLIMATE CHANGE. Geophysical Research Letters 32, no. 19: n/a-n/a. https://doi.org/10.1029/2005GL023653.

Boxhammer, T., Bach, L.T., Czerny, J., Riebesell, U., 2016. Technical note: Sampling and processing of mesocosm sediment trap material for quantitative biogeochemical analysis. Biogeosciences 13, 2849–2858. https://doi.org/10.5194/bg-13-2849-2016

Brander, Keith, 2010. Impacts of Climate Change on Fisheries. Journal of Marine Systems 79, no. 3–4: 389–402. https://doi.org/10.1016/j.jmarsys.2008.12.015.

Brzezinski, Ma, Rj Olson, and Sw Chisholm, 1990. Silicon Availability and Cell-Cycle Progression in Marine Diatoms. Marine Ecology Progress Series 67: 83–96. https://doi.org/10.3354/meps067083.

Brzezinski, M. A. 1992. Cell-cycle effects on the kinetics of silicic acid uptake and resource competition among diatoms. J. Plankton Res. 14:1511–39.

Brzezinski, Mark A, 2004. THE Si:C:N RATIO OF MARINE DIATOMS: INTERSPECIFIC VARIABILITY AND THE EFFECT OF SOME ENVIRONMENTAL VARIABLES1. Journal of Phycology 21, no. 3: 347–57. https://doi.org/10.1111/j.0022-3646.1985.00347.x.

Claquin, P., Martin-Jézéquel, V., Kromkamp, J. C., Veldhuis, M. J. W., and Kraay, G. W, 2002. Uncoupling of silicon compared with carbon and nitrogen metabolisms and the role of the cell cycle in continuous cultures of Thalassiosira pseudonana (Bacillariophyceae) under light, nitrogen, and phosphorus control, J. Phycol., 38, 922–930.

Cushing DH, 1989. A difference in structure between ecosystems in strongly stratified waters and in those that are only weakly stratified. J Plankton Res 11:1–13

De León, A.R. and J.G. Braun, 1973. Ciclo anual de la produccion primaria y su relación con los nutrientes en aguas Canarias. Bol. Inst. Esp. Ocean., 167: 1-24

Diaz R J, Rosenberg R.2008. Spreading dead zone sand consequences for marine ecosystems. Science 321:926– 29

Dutz, J., Koski, M., Jónasdóttir, S.H., 2008. Copepod reproduction is unaffected by diatom aldehydes or lipid composition. Limnol. Oceanogr. 53, 225–235.

Eppley RW, Peterson BJ, 1979. Particulate organic matter flux and planktonic new production in the deep ocean. Nature 282:677–680

Fingas, Merv, 2019. 'Remote Sensing for Marine Management'. In World Seas: An Environmental Evaluation, 103–19. Elsevier. https://doi.org/10.1016/B978-0-12-805052-1.00005-X.

Fuller, R.D., 1978. Ocean thermal energy conversion. Ocean Management, Oceanology international "78 4, 241–258. https://doi.org/10.1016/0302-184X(78)90026-4

Giraud, M., Boye, M., Garçon, V., Donval, A., de la Broise, D., 2016. Simulation of an artificial upwelling using immersed in situ phytoplankton microcosms. Journal of Experimental Marine Biology and Ecology 475, 80–88. https://doi.org/10.1016/j.jembe.2015.11.006

Handå, A., McClimans, T.A., Reitan, K.I., Knutsen, Ø., Tangen, K., Olsen, Y., 2013. Artificial upwelling to stimulate growth of non-toxic algae in a habitat for mussel farming. Aquaculture Research n/a-n/a. https://doi.org/10.1111/are.12127

Humborg 0C, I ttekkot V, Cociasu A, von Bodungen B. 1997. Effect of Danube river damon Black Sea biogeochemistry and ecosystem structure. Nature 386:385–88

Humborg C, Conley DJ, Rahm L, Wulff F, Cociasu A, Ittekkot V. 2000. Silicon retention in river basins: far-reaching effects on biogeochemistry and aquatic food webs in coastal marine environments. Ambio 29:45–50

Ianora, A., Poulet, S.A., Miralto, A., 1995. A comparative study of the inhibitory effect of diatoms on the reproductive biology of the copepod Temora stylifera. Mar. Biol. 121, 533–539

Irigoien, X., et al., 2002. Copepod hatching success in marine ecosystems with high diatom concentrations. Nature 419, 387–389. http://dx.doi.org/10.1038/nature01055.

Ittekkot V, Humborg C, Sch¨afer P. 2000. Hydrological alternations and marine biogeochemistry: a silicate issue? BioScience 50:776–82

J. Monod, 1942. Recherches sur croissance des cultures bacteriennes [studies on the growth of bacterial cultures] Actual. Sci. Ind., 9111-215

Jónasdóttir, S.H., Kiørboe, T., 1996. Copepod recruitment and food composition: do diatoms affect hatching success? Mar. Biol. 125, 743–750

Jónasdóttir, S.H., Kiørboe, T., Tang, K.W., St. John, M.A., Visser, A.W., Saiz, E., Dam, H.G., 1998. Role of diatoms in copepod production: good, harmless or toxic? Mar. Ecol. Prog. Ser. 172, 305–308.

Keller, D.P., Feng, E.Y., Oschlies, A., 2014. Potential climate engineering effectiveness and side effects during a high carbon dioxide-emission scenario. Nature Communications 5. https://doi.org/10.1038/ncomms4304

Lenton, T.M., Vaughan, N.E., 2009. The radiative forcing potential of different climate geoengineering options. Atmos. Chem. Phys. 9, 5539–5561. https://doi.org/10.5194/acp-9-5539-2009

Liu, Hongbin, Mianrun Chen, Feng Zhu, and Paul J. Harrison, 2016. Effect of Diatom Silica Content on Copepod Grazing, Growth and Reproduction. Frontiers in Marine

Science 3. https://doi.org/10.3389/fmars.2016.00089.

Liu, Hongbin, and Chih-Jung Wu, 2016. Effect of the Silica Content of Diatom Prey on the Production, Decompositionand Sinking of Fecal Pellets of the Copepod Calanus Sinicus. Biogeosciences 13, no. 16: 4767–75. https://doi.org/10.5194/bg-13-4767-2016.

Mann, David G, 1999. The Species Concept in Diatoms. Phycologia 38, no. 6: 437–95. https://doi.org/10.2216/i0031-8884-38-6-437.1.

Martin-Jezequel, Veronique, Mark Hildebrand, and Mark A. Brzezinski, 2000. SILICON METABOLISM IN DIATOMS: IMPLICATIONS FOR GROWTH. Journal of Phycology 36, no. 5: 821–40. https://doi.org/10.1046/j.1529-8817.2000.00019.x.

McAndrew, P., Björkman, K., Church, M., Morris, P., Jachowski, N., Williams PJ, leB, Karl, D., 2007. Metabolic response of oligotrophic plankton communities to deep water nutrient enrichment. Marine Ecology Progress Series 332, 63–75. https://doi.org/10.3354/meps332063

McClimans, T.A., Handå, A., Fredheim, A., Lien, E., Reitan, K.I., 2010. Controlled artificial upwelling in a fjord to stimulate non-toxic algae. Aquacultural Engineering 42, 140– 147. https://doi.org/10.1016/j.aquaeng.2010.02.002

McNair, Heather M., Mark A. Brzezinski, and Jeffrey W. Krause, 2018. Diatom Populations in an Upwelling Environment Decrease Silica Content to Avoid Growth Limitation: Diatom Physiology and Silicon Stress. Environmental Microbiology 20, no. 11: 4184–93. https://doi.org/10.1111/1462-2920.14431.

Miralto, A., Barone, G., Romano, G., Poulet, S.A., et al., 1999. The insidious effect of diatoms on copepod reproduction. Nature 402, 173–176.

Moore, C. M., M. M. Mills, K. R. Arrigo, I. Berman-Frank, L. Bopp, P. W. Boyd, E. D. Galbraith, et al., 2013. Processes and Patterns of Oceanic Nutrient Limitation. Nature Geoscience 6, no. 9: 701–10. https://doi.org/10.1038/ngeo1765.

Muller-Karger, Frank E, 2005. The Importance of Continental Margins in the Global Carbon Cycle. Geophysical Research Letters 32, no. 1: L01602. https://doi.org/10.1029/2004GL021346.

Nelson, David M., Paul Tréguer, Mark A. Brzezinski, Aude Leynaert, and Bernard Quéguiner, 1995. Production and Dissolution of Biogenic Silica in the Ocean: Revised Global Estimates, Comparison with Regional Data and Relationship to Biogenic Sedimentation. Global Biogeochemical Cycles 9, no. 3: 359–72. https://doi.org/10.1029/95GB01070.

Nelson DM, Dortch Q. 1996. Silicic acid depletion and silicon limitation in the plume of the Mississippi River: evidence from kinetic studies in spring and summer. Mar. Ecol. Prog. Ser. 136:163–78

O'Connor MI, Piehler MF, Leech DM, Anton A, Bruno JF. 2009. Warming and resource availability shift food web structure and metabolism. PLoS Biol. 7:e1000178

Pančić, Marina, Rocio Rodriguez Torres, Rodrigo Almeda, and Thomas Kiørboe, 2019. Silicified Cell Walls as a Defensive Trait in Diatoms. Proceedings of the Royal Society B: Biological Sciences 286, no. 1901: 20190184. https://doi.org/10.1098/rspb.2019.0184.

Pelegrı´, J.L., Marrero-Dı´az, A., Ratsimandresey, A.W., Antoranz, A., Cisneros-Aguirre, J., Gordo, C., Grisolı´a, D., Herna´ndezGuerra, A., La´iz, I., Martı´nez, A., Parrilla, G., Pe´rez-Rodrı´guez, P., Rodrı´guez-Santana, A., Sangra`, P., 2005. Hydrographic cruises off northwest Africa: the Canary Current and the Cape Ghir filament. J. Mar. Syst. 54, 39–63 (this issue).

'Poulet, S.A., Ianora, A., Miralto, A., Meijer, L., 1994. Do diatoms arrest egg development in copepods? Mar. Ecol. Prog. Ser. 111, 79–86.

A. C. Redfield. B. H. Ketchum and F. A. Richards, 1960. THE INFLUENCE OF ORGANISMS ON THE COMPOSITION OF SEA-WATER.:26-72

Sarmiento, Jorge L., and Nicolas Gruber, 2002. Sinks for Anthropogenic Carbon. Physics Today 55, no. 8: 30–36. https://doi.org/10.1063/1.1510279.

Schmitz, William J., and Michael S. McCartney, 1993. On the North Atlantic Circulation. Reviews of Geophysics 31, no. 1: 29–49. https://doi.org/10.1029/92RG02583.

Sharp, J.H. 1974. Improved analysis for particulate organic carbon and nitrogen from seawater. Limnol. Oceanogr., 19: 984 – 989.

Smetacek V, 1999. Diatoms and the ocean carbon cycle. Protist 150: 25−32

Sommer U, 1983. Nutrient competition between phytoplankton in multispecies chemostat experiments. Arch Hydrobiol 96:399-416

Sommer U, 1994. Planktologie. Springer, Berlin Heidelberg New York

Sommer U, 1996. Plankton ecology: the past two decades of progress. Naturwissenschaften 83:293-301

Sommer, U., 1998. Silicate and the functional geometry of marine phytoplankton. J. Plankton Res. 20, 1853 – 1859.

Sommer, Ulrich, Herwig Stibor, Alexis Katechakis, Frank Sommer, and Thomas Hansen, 2002. Pelagic Food Web Configurations at Different Levels of Nutrient Richness and Their Implications for the Ratio Fish Production:Primary Production. In Sustainable Increase of Marine Harvesting: Fundamental Mechanisms and New Concepts, edited by Olav Vadstein and Yngvar Olsen, 11–20. Dordrecht: Springer Netherlands. https://doi.org/10.1007/978-94-017-3190-4_2.

Steinacher M, Joos F, Froelicher TL, Bopp L, Cadule P, et al.2010. Projected 21 st century decrease in marine productivity: a multi-model analysis. Biogeosciences 7:979–1005

Strohmeier, T., Strand, ø, Alunno-Bruscia, M., Duinker, A., Rosland, R., Aure, J., Erga, S.,Naustvoll, L., Jansen, H., Cranford, P., 2015. Response of Mytilus edulis to enhanced phytoplankton availability by controlled upwelling in an oligotrophic fjord. Marine Ecology Progress Series 518, 139–152. https://doi.org/10.3354/meps11036

Taylor F.J.R. & Pollingher U. 1987. Ecology of dinoflagellates. In: The biology of dinoflagellates (Ed. By F.J.R. Taylor), pp. 398-502. Blackwell Scientist, Palo Alto, CA, USA.

Taucher, Jan, Lennart T. Bach, Tim Boxhammer, Alice Nauendorf, Eric P. Achterberg, María Algueró-Muñiz, Javier Arístegui, et al, 2017. Influence of Ocean Acidification and Deep Water Upwelling on Oligotrophic Plankton Communities in the Subtropical North Atlantic: Insights from an In Situ Mesocosm Study. Frontiers in Marine Science 4. https://doi.org/10.3389/fmars.2017.00085.

Thamatrakoln, Kimberlee, and Mark Hildebrand, 2008. Silicon Uptake in Diatoms Revisited: A Model for Saturable and Nonsaturable Uptake Kinetics and the Role of Silicon Transporters. Plant Physiology 146, no. 3: 1397–1407. https://doi.org/10.1104/pp.107.107094.

Tilman D, 1982. Resourses competition and community structure. Princeton UniversityPress, Princeton

Tilman D, Kiesling R, Sterner R, Kilham SS, Johnsen FA, 1986. Green, bluegreen and diatom algae: taxonomic differences in competitive ability for phosphorus, silicon and nitrogen. Arch Hydrobiol 106:473-485

Tréguer, P, Nelson, DM, Bennekom, AJ, Demaster, DJ, Leynaert, A and Queguiner, B. 1995. The silica balance in the world ocean: a re-estimate. Science, 268: 375–379

Tréguer, Paul J., and Christina L. De La Rocha, 2013. The World Ocean Silica Cycle. Annual Review of Marine Science 5, no. 1: 477–501. https://doi.org/10.1146/annurev-marine-121211-172346.

Tréguer, Paul, and Philippe Pondaven, 2000. Silica Control of Carbon Dioxide. Nature 406, no. 6794: 358–59. https://doi.org/10.1038/35019236.

Turner RE, Rabalais NN. 1994.Coastal eutrophication near the Mississippi River Delta.Nature 368:619–21

Ulrich Sommer, Herwig Stibor, Alexis Katechakis, Frank Sommer and Thomas Hansen, 2002.Pelagic food web configurations at different levels of nutrient richness and their implications for the ratio fish production:primary production" Hydrobiologia 484: 11–20.

Van Nieuwerburgh, Lies, Ingrid Wänstrand, and Pauli Snoeijs, 2004. Growth and C:N:P Ratios in Copepods Grazing on N- or Si-Limited Phytoplankton Blooms. Hydrobiologia 514, no. 1–3: 57–72. https://doi.org/10.1023/B:hydr.0000018206.02271.2b.

Volk, T., Hoffert, M. I, 1984. Ocean carbon pumps: analysis of relative strengths and efficiencies in ocean-driven atmospheric CO2 changes**.** The carbon cycle and

atmospheric CO 2: natural variations Archean to present. Chapman conference papers,. editor E.T. Sundquist; W.S. Broecker. American Geophysical Union; Geophysical Monograph 32, 1985. pp. 99-110

Wichard, T., Poulet, S.A., Boulesteix, A., Ledoux, J.B., Lebreton, B., Marchetti, J., Pohnert G., 2008. Influence of diatoms on copepod reproduction. II. Uncorrelated effects of diatom-derived, α,β,γ,δ-unsaturated aldehydes and polyunsaturated fatty acids on Calanus helgolandicus in the field. Prog. Oceanogr. 77, 30–44.

Williamson, N., Komiya, A., Maruyama, S., Behnia, M., Armfield, S.W., 2009. Nutrient transport from an artificial upwelling of deep sea water. Journal of Oceanography 65, 349–359. https://doi.org/10.1007/s10872-009-0032-x

Wolf-Gladrow, Dieter A., Richard E. Zeebe, Christine Klaas, Arne Körtzinger, and Andrew G. Dickson, 2007. 'Total Alkalinity: The Explicit Conservative Expression and Its Application to Biogeochemical Processes'. Marine Chemistry 106, no. 1–2: 287–300. https://doi.org/10.1016/j.marchem.2007.01.006.

Yool, A., Shepherd, J.G., Bryden, H.L., Oschlies, A., 2009. Low efficiency of nutrient translocation for enhancing oceanic uptake of carbon dioxide. Journal of Geophysical Research 114. https://doi.org/10.1029/2008JC004792

Zehr, Jonathan P, John B Waterbury, Patricia J Turner, Joseph P Montoya, Enoma Omoregie, Grieg F Steward, Andrew Hansen, and David M Karl, 2001. Unicellular Cyanobacteria ®x N2 in the Subtropical North Paci®c Ocean 412: 4.

https://www.ipcc.ch/report/ar5/syr/

https://report.ipcc.ch/sr15/pdf/sr15_spm_final.pdf

http://www.ncdc.noaa.gov/cag/time-series/global/globe/ocean/ytd/12/1880-2016.

https://www.offshoreengineering.com/education/oceanography